Continental Shelf Research, Vol. 11, Nos 8–10, pp. 977–1012, 1991.
Printed in Great Britain.

0278-4343/91 $3.00 + 0.00

Mean circulation and variability on the eastern Canadian continental shelf

PETER C. SMITH* and FRANKLIN B. SCHWING†

(*Received* 22 *January* 1990; *in revised form* 1 *August* 1990; *accepted* 6 *December* 1990)

Abstract—The circulation and variability on eastern Canadian continental shelves is reviewed with emphasis on horizontal and vertical structure in the water column. Mean and seasonal currents, sheared by stratification and friction, generally follow bathymetry and are driven primarily by surface wind stress and buoyancy fluxes. In certain near-resonant embayments, nonlinear interactions of the tide also make significant contributions to the mean and low-frequency currents. Direct forcing of low-frequency shelf circulation by offshore currents and pressure fields is of lesser importance according to recent observations and models. At higher frequencies, the wintertime response to atmospheric forcing occurs in three important frequency bands: surface wave (periods of 2–20 s), inertial (17–22 h) and synoptic or subtidal (2–10 days). Most of the subtidal energy in the subsurface pressure (SSP) field is attributable to direct local forcing by alongshore wind and to remote forcing by coastal-trapped waves (CTW). The subtidal current variability is less coherent with these sources primarily because of small scale circulations created by vortex stretching, topographic steering and scattering by the rugged shelf bathymetry. Bottom friction and scattering control the ratio of locally and remotely forced subtidal energy as a function of position on the shelf. Intermittent inertial currents in stratified shelf waters, often associated with mesoscale atmospheric forcing, exhibit a 180° phase change across the pycnocline and are inhibited near the coast. Surface waves generated by storm winds are strongly dissipated in shallow water, where they enhance bottom stresses that: (1) balance the surface wind stress; and (2) may contribute to the damping of inertial waves. Specific examples of these phenomena are drawn from observations on the Scotian Shelf and in the Gulf of Maine.

INTRODUCTION

THE continental margin of eastern Canada is characterized by broad shelves (100–200 km) with rugged topography, separated from the abyssal depths by a steep continental slope. Deep basins and marginal troughs (>200 m) are typically found in the nearshore regions of the shelf, whereas long chains of shallow banks in the offshore regions often create a natural barrier to exchanges between oceanic and coastal waters. The coastline is also quite irregular, punctuated by several large gulfs and embayments (for example Gulf of Maine, Gulf of St Lawrence, Hudson Strait; Fig. 1a). All of these physical features have important consequences for the structure and variability of the coastal circulation.

* Physical and Chemical Sciences, Department of Fisheries and Oceans, Bedford Institute of Oceanography, Dartmouth, Nova Scotia, Canada.

† Pacific Fisheries Environmental Group, Southwest Fisheries Center, NMFS, NOAA, Monterey, California, U.S.A.

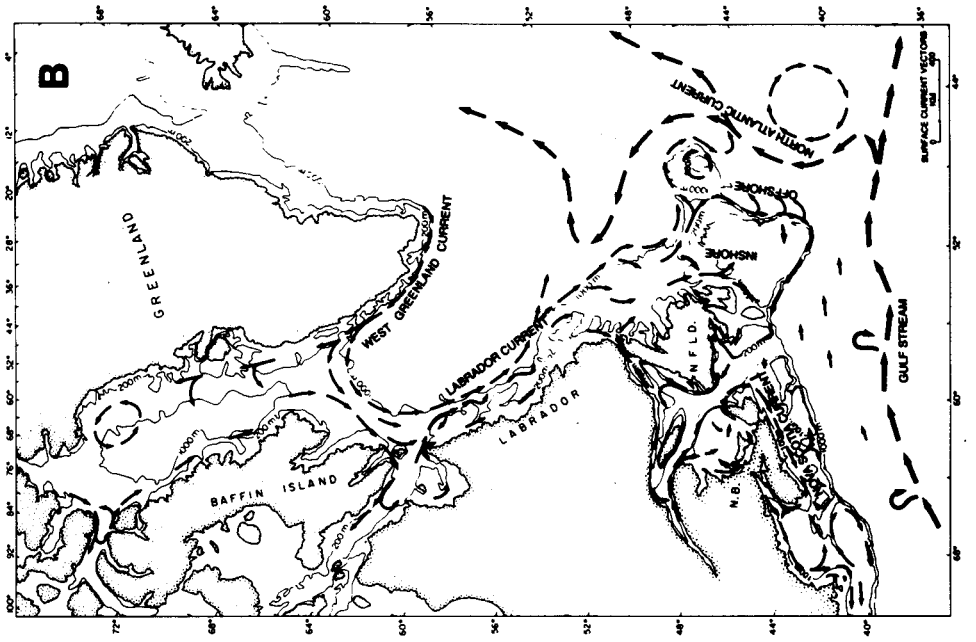
B
GREENLAND
WEST GREENLAND CURRENT
LABRADOR CURRENT
BAFFIN ISLAND
LABRADOR
NFLD.
N.B.
NORTH ATLANTIC CURRENT
OFFSHORE
INSHORE
GULF STREAM
SURFACE CURRENT VECTORS

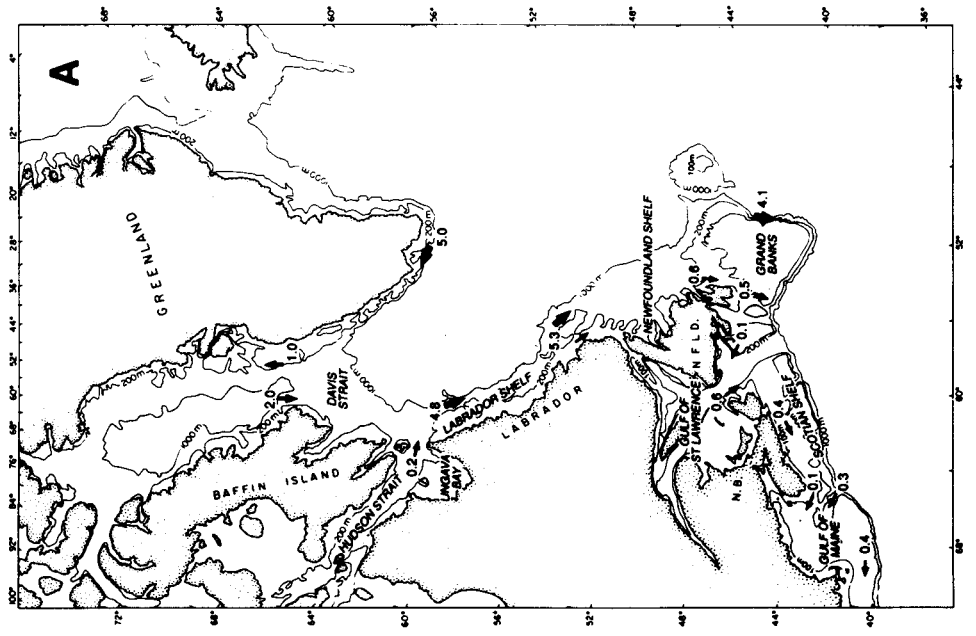
A
GREENLAND
DAVIS STRAIT
BAFFIN ISLAND
HUDSON STRAIT
LABRADOR SHELF
LABRADOR
NEWFOUNDLAND SHELF
GRAND BANKS
GULF OF ST LAWRENCE
NFLD.
N.B.
SCOTIAN SHELF
GULF OF MAINE

Potentially important driving forces for the coastal circulation include the surface wind stress, tidal forces, buoyancy fluxes and the large-scale circulation associated with adjacent deep ocean gyres. Wind stress influences the flow on a wide range of time scales from the steady mean currents to the order of seconds for surface gravity waves. In winter, wind-driven circulation often dominates in two frequency bands: (1) the synoptic band (periods of 2–10 days) associated with severe storms; and (2) the inertial band (periods of 17–22 h; SMITH *et al.*, 1978). Surface gravity waves generated by winter storms also have a significant effect on the low-frequency circulation (and the seabed) in shallow water through their enhancement of bottom shear stress (GRANT and MADSEN, 1979). However, in southern regions such as the Scotian Shelf, the mean wind stress (eastward) opposes the mean shelf current (southwest). This fact led CSANADY (1976) to conclude that an alongshore pressure gradient of some other origin must drive the mean flow. But recent studies (BRINK, 1986; HAIDVOGEL and BRINK, 1986) suggest that rectification of wind-driven current fluctuations by topographic drag asymmetries may contribute to the mean flow in the direction of CTW propagation (southwest).

Buoyancy fluxes associated with large freshwater inputs to the coastal zone produce strong density gradients leading to alongshore pressure gradients that drive alongshore current (CSANADY, 1976; 1978). Baroclinicity can also interact with shelf–slope topography through the so-called JEBAR effect (Joint Effect of Baroclinicity and Relief; SHAW and CSANADY, 1983; HUTHNANCE, 1984; WEAVER and HSIEH, 1987) to induce depth-averaged advection on the shelf. These mechanisms generally operate at very long time scales (seasonal or greater), consistent with the freshwater forcing cycles.

Offshore forcing has also been proposed as the origin of the alongshore pressure gradient that drives the mean flow on the shelf. BEARDSLEY and WINANT (1979) concluded that local buoyancy fluxes were insufficient forcing on the U.S. east coast and that the required pressure gradient originates as a boundary effect of the large-scale circulation. However, more recent studies (WANG, 1982; CSANADY and SHAW, 1983) have used barotropic models to demonstrate the "insulating" effect of the continental slope which traps the effects of large-scale pressure gradients over the upper slope and prevents them from penetrating onto the shelf. Furthermore, results of a stratified steady model (KELLY and CHAPMAN, 1988) have shown that the effects of reasonable stratification and vertical structure of the imposed pressure field are unable to break this topographic constraint, although they do have a significant impact on the distribution of energy over the slope.

On a smaller scale, offshore eddies and rings have an important influence on the circulation over the slope and rise. Gulf Stream warm-core rings, for example, entrain large quantities of coastal water from the Scotian Shelf (SMITH, 1978), while interactions between the Labrador Current and eddies of the North Atlantic Current system are probably responsible for the high rate of loss of surface drifters along the southeastern flank of the Grand Banks of Newfoundland (PETRIE and ANDERSON, 1983; GREENBERG and PETRIE, 1988). When a Gulf Stream ring suddenly encounters a sloping bottom, it radiates low-frequency energy in the form of topographic Rossby waves with characteristic periods

Fig. 1. (A) Estimates of volume transport on the continental shelf off eastern Canada. Numbers represent transport in units of 10^6 m^3 s^{-1} (after CHAPMAN and BEARDSLEY, 1989). (B) Qualitative estimation of the surface circulation off eastern Canada (see GREENBERG and PETRIE, 1988).

of 10–30 days (LOUIS and SMITH, 1982; LOUIS *et al.*, 1982). On approach to the shelf, however, the wave energy is strongly refracted by the continental slope and scattered into baroclinic modes trapped to the shelf edge such that little energy penetrates onto the shelf (SMITH, 1983a). Furthermore, frictional dissipation limits the influence of the waves on the shelf circulation. CHAPMAN and BRINK (1987) have used a linear, stratified model to examine the shelf and slope circulations induced by periodic offshore forcing and conclude that, at the energetic deep ocean time scales (periods greater than 10 days), the shelf response is inevitably weak and barotropic. In addition, the response to a single translating eddy (with realistic vertical structure) moving close to the slope is blocked by the topography and "squashed" at the shelf break. Only a very weak circulation cell is induced over the shelf. Thus, the consensus appears to be that offshore forcing does not have an important influence on the general circulation of the shelf at low frequencies. Nevertheless, eddies do affect near-bottom currents, stress and sediment transport near the shelf break, i.e. at depths of 200–400 m (BUTMAN, 1987).

The dynamics of the "first-order" barotropic tidal circulation on the continental shelf are reasonably well understood through the calibration and verification of numerical models (e.g. PETRIE *et al.*, 1987a). Furthermore, geometries such as the Gulf of Maine/Bay of Fundy (GREENBERG, 1983) and Ungava Bay (GRIFFITHS *et al.*, 1981) produce near-resonant responses at semidiurnal frequencies such that: (1) tidal currents dominate local kinetic energy budgets; and (2) significant residual mean, monthly, fortnightly and higher harmonic (shallow water tidal) circulations develop through nonlinear interaction (LODER, 1980). In shallow regions, such as Georges Bank and the inner Bay of Fundy, the tidal currents vertically mix the water column and largely govern the resuspension of bottom sediment (BUTMAN, 1987; AMOS and JUDGE, this issue). Under these conditions, barotropic models permit reasonable simulations of sediment transport and deposition (GREENBERG and AMOS, 1983).

On the other hand, the dynamics of the tidally-induced residual flow field in deeper areas are not well known, nor are the flows themselves easily determined by observations (TEE *et al.*, 1988). Furthermore, in order to model shelf circulation processes properly, the rates of dissipation and mixing of momentum and density must be accurately specified. For example, WRIGHT and LODER (1988) have shown that model estimates of topographic rectification of tidal currents are sensitive to the parameterization scheme for bottom friction. This uncertainty frustrates attempts to compare model results to observations. Similarly, spatial variations in the strength of a linear bottom friction coefficient can have a significant impact on the structure of the wind-driven response (CLARKE and BRINK, 1985) or on the downstream evolution of the barotropic mean flow on the shelf (CHAPMAN *et al.*, 1986).

This review will be focused on recent advances in understanding certain aspects of the circulation on the continental shelves of Atlantic Canada. Some simple, linear, barotropic models are first examined. The mean and seasonal circulation patterns will then be presented followed by a description of wind-driven variability. Emphasis throughout will be placed on the vertical and horizontal structure of flow fields. The direct effects of offshore forcing will not be considered further because of its generally weak influence on the shelf circulation. Moreover, in spite of their dominance in some regimes, tidal currents will be largely ignored. Finally, though the physical processes discussed are generally found over the entire eastern shelf region, specific examples are drawn primarily from two experiments conducted on the Scotian Shelf: the Cape Sable Experiment, 1979–1980

(SMITH, 1983b) and the Canadian Atlantic Storms Program (CASP, December 1985–April 1986; ANDERSON and SMITH, 1989).

SIMPLE DYNAMICAL MODELS

From the wealth of recent observations, a number of important concepts have emerged to explain the primary dynamical balances in the mean and low-frequency circulation of the coastal ocean (CSANADY, 1982). Following WRIGHT (1986), the linearized, shallow water hydrodynamic equations may be derived under the assumptions that the homogeneous fluid layer is thin (hydrostatic) and that weak velocities render the convective accelerations much smaller than the Coriolis terms:

$$u_t - fv = -g\zeta_x - \frac{ru}{h}, \tag{1}$$

$$v_t + fu = -g\zeta_y - \frac{rv}{h} + \frac{\tau^y}{\rho h}, \tag{2}$$

$$(hu)_x + (hv)_y = \zeta_t, \tag{3}$$

where the subscripts denote differentiation, (u, v) are the depth-averaged horizontal velocity components in the x (cross-shore) and y (alongshore) directions, $z = -h(x, y)$ is the bottom and $z = \zeta(x, y, t)$ is the position of the sea surface. The flow is forced by the alongshore wind stress component, $\tau^y(x, y, t)$, and retarded by linear bottom friction,

$$\text{bottom stress} = \rho(ru, rv) \tag{4}$$

where $r(x, y)$ is a spatially-varying resistance coefficient.

For harmonic time dependence $[\zeta(x, y, t) = Re(\bar{\zeta}(x, y)e^{-i\omega t})]$, (1)–(3) may be reduced to a single equation

$$-h_x\bar{\xi}_y + h_y\bar{\xi}_x = f^{-1}[(r - i\omega h)\bar{\xi}_x]_x \tag{5}$$

with the coastal boundary condition of no normal transport

$$h\bar{\xi}_y + f^{-1}(r - i\omega h)\bar{\xi}_x = \frac{\bar{\tau}^y}{\rho g} \qquad \text{at } x = 0 \tag{6}$$

under the following reasonable assumptions for the shelf setting

$$(\omega/f)^2 \ll 1 \qquad \text{low frequency} \tag{7a}$$

$$(r/fh)^2 \ll 1 \qquad \text{weak friction} \tag{7b}$$

$$(L_x/L_y)^2 \ll 1 \qquad \text{long wave approximation} \tag{7c}$$

$$(L_x/\lambda_e)^2 \ll 1 \qquad \text{rigid lid} \tag{7d}$$

$$L_x/L_\tau \ll 1 \qquad \text{uniform forcing} \tag{7e}$$

where L_x, L_y are the scales of variation in the cross-shelf and alongshore directions, $\lambda_e = \sqrt{gh}/f$ is the external Rossby deformation scale and L_τ is the scale for variations in the wind field. With certain further simplifications, equations (5) and (6) have spawned a

number of illustrative models whose basic character is dictated by the parameter, $r/\omega h$, the ratio of the forcing time scale (ω^{-1}) to the frictional spindown time (h/r).

The quasisteady limit ($r/\omega h \gg 1$) with plane beach topography [$h = h(x)$, $h_x = s$ = constant] and constant r leads to CSANADY's (1978, 1981) "arrested topographic wave" (ATW) solutions. Two canonical solutions for such an idealized shelf region are obtained by analogy with one-dimensional heat conduction. First of all, in the absence of wind ($\tau^y = 0$), the pressure field resulting from a coastal mass source applied at a particular cross-shelf transect (the "backward boundary")

$$\bar{\zeta} = \zeta_o(x) = M\delta(x) \qquad \text{at } y = 0 \tag{8}$$

"diffuses" away from the coast for increasing values of the time-like variable, $-y$. The solutions for sea level and depth-averaged alongshore current are given by (CSANADY, 1981)

$$\bar{\zeta}_Q(x, y) = \left(\frac{2}{\pi}\right)^{1/2} \frac{M}{L_x} e^{-\xi^2} \tag{9a}$$

$$\bar{v}_Q(x, y) = -\frac{2}{\pi^{1/2}} \left(\frac{fQ}{2ry}\right) \xi e^{-\xi^2} \tag{9b}$$

where

$$L_x = (-2ry/fs)^{1/2} \tag{10}$$

is the cross-shelf scale of the coastal boundary layer, $\xi = x/2^{1/2}L_x$, and $Q = -gsM/f$ is the volumetric alongshore transport. The effective diffusivity is r/fs and, because of the parabolic nature of the equation, the distribution imposed at $y = 0$ affects the shelf circulation only in the "forward" direction ($y < 0$) in the sense of shelf wave propagation.

On the other hand, when the boundary forcing is absent [$\zeta = \zeta_o(x) = 0$ at $y = 0$], the solution for steady wind forcing over a limited portion of the shelf

$$\frac{\tau^y}{\rho} = \begin{cases} F, & y < 0 \\ 0, & y > 0 \end{cases} \tag{11}$$

is given by (CSANADY, 1978)

$$\bar{\zeta}_W = -\left(\frac{2}{\pi}\right)^{1/2} \frac{fF}{rg} L_x \{e^{-\xi^2} - \pi^{1/2}\xi erfc(\xi)\} \tag{12a}$$

$$\bar{v}_W = \frac{F}{r} erfc(\xi). \tag{12b}$$

Again a coastal boundary layer of scale, L_x, grows in the $y < 0$ direction as it absorbs or emits the cross-shelf Ekman flux associated with the alongshore wind.

The normalized cross-shelf profiles of depth-averaged alongshore current are plotted in Fig. 2a as a function of the scaled variable, $\xi(x, y) = x/2^{1/2}L_x(y)$. The boundary-driven current vanishes at the coast along with ζ_x and achieves a maximum value at $x = L_x$. Close to shore, the alongshore gradient, ζ_y, drives the flow against friction, while offshore ($x > L_x$), the gradient changes sign as the Coriolis force of the cross-shore transport becomes important. In contrast, the wind-forced current is maximum at the coast, where

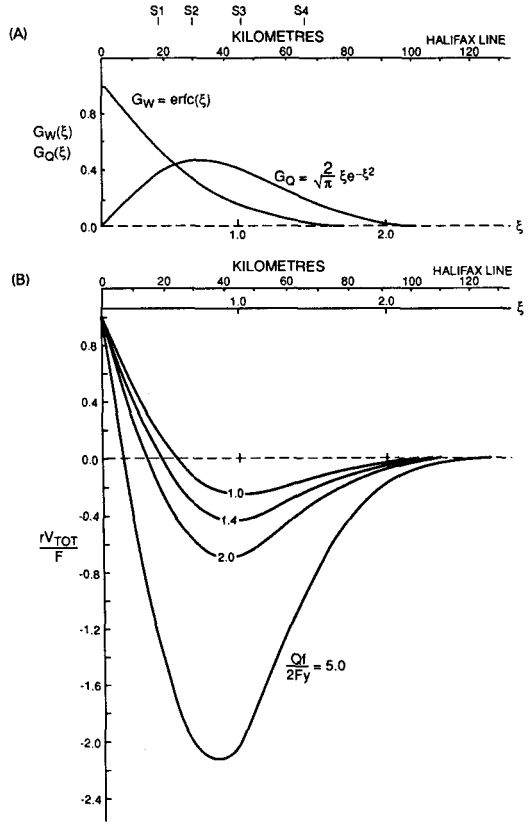

Fig. 2. (A) Cross-shelf structure functions for alongshore velocity from the frictional barotropic models on a plane beach: $G_W(\xi)$ for the local wind-forced solution (12b) and $G_Q(\xi)$ for the boundary-forced solution (9b). (B) Scaled distribution for the cross-shelf profile of alongshore current as a function of downshelf distance in the forward direction.

surface and bottom stresses balance as $h \Rightarrow 0$, and decreases monotonically in the offshore direction.

On a typical east coast shelf, the mean flow is subject to both wind and boundary forcing. By virtue of linearity, the solutions (9) and (12) may be added to give an estimate of the combined alongshore flow resulting from the two forcings

$$\bar{v}_{TOT} = \bar{v}_W + \bar{v}_Q = \frac{F}{r} erfc(\xi) - \frac{2}{\pi^{1/2}}\left(\frac{fQ}{2ry}\right)\xi e^{-\xi^2} = \frac{F}{r}[G_W(\xi) - KG_Q(\xi)] \qquad (13)$$

where $G_W(\xi) = erfc(\xi)$, $G_Q(\xi) = 2/\pi^{1/2}\xi e^{-\xi^2}$ and $K = fQ/2Fy$. For constant Q and F of opposite sign, the value of K, representing the relative influence of the boundary-forced flow, diminishes with increasingly negative y (Fig. 2b). This results in a nearshore flow reversal which migrates offshore within the scaled boundary layer structure. Of course, by virtue of that scaling, the streamlines are also migrating offshore as $(-y)^{1/2}$.

WANG (1982) solved numerically a somewhat more complicated steady problem with a segmented shelf/slope topography, offshore forcing ($\zeta_y = \gamma$ = constant at $x = W$) and alongshore depth variation [$h = h(x, y)$] to demonstrate the insulating effect of the continental slope and the channelling effect it has on the alongshore flow. CHAPMAN *et al.* (1986) used a similar model with weaker variable friction [$r = r(x)$] to demonstrate that the unusually rapid shift of Wang's coastal current to the slope region was a consequence of his specification of a large, constant value of r. In another paper, CHAPMAN (1986) also demonstrates that the cross-shelf convergence associated with shelf/slope topography and variable friction is capable of maintaining a front in the distribution of a passive tracer near the shelf break. WRIGHT (1989) then showed that a similar mechanism operates even when there is a significant density contrast across the front; that is, friction will cause the front to migrate across the shelf region, then "stall" in the vicinity of the shelf break.

In the very weak friction limit ($r/\omega h \ll 1$), equations (5) and (6) result in damped Rossby waves either locally forced or propagating into the domain as free waves from the backward boundary (GILL and SCHUMANN, 1974). Weak friction acts to damp the free wave amplitudes in the forward direction and produce phase shifts between the nearshore and offshore fluctuations, whereas for forced waves, the phase difference between the stress and velocity is reduced by friction (BRINK and ALLEN, 1978; WRIGHT, 1986).

For constant r and frequency, ω, the parameter $r/\omega h$ increases shoreward on a constant sloping bottom. Comparing the zone where $r/\omega h \gg 1$ with the ATW trapping zone, $x < L$, WRIGHT (1986) concluded that arrested topographic wave dynamics are strictly applicable only at very low frequencies,

$$\omega/f \ll rl/2h_x\omega \cong 10^{-2}$$

where l is the wave number for periodic forcing. However SCHWING (1989a) has demonstrated that the time-dependent ATW solution (ATW spatial pattern with harmonic time dependence) is useful at much higher frequencies, well into the wind forced band.

MEAN AND SEASONAL CIRCULATION

Mean circulation

CHAPMAN and BEARDSLEY (1989) have suggested that the mean circulation off Canada's east coast is part of a 5000 km buoyancy-driven coastal current which originates off the southern coast of Greenland. They base this proposal on oxygen isotope data which show that the freshwater component of the shelf water as far south as the Middle Atlantic Bight (off the eastern U.S.) is highly depleted in ^{18}O. The isotopic content is similar to that of local glacial melt and river runoff into the northern Labrador Sea, suggesting that the associated buoyancy fluxes may be important driving forces for the coastal flow. This hypothesis is consistent with most of the known features of the mean circulation (Fig. 1). The measured (or inferred) transports and the estimated surface currents indicate that the dominant component of the flow follows the west coast of Greenland, then splits near the sill in Davis Strait with the southern branch feeding the flow onto the Labrador Shelf. The southward flow accelerates (to 0.4–0.6 m s^{-1}) as it passes Hudson Strait due to bathymetric convergence and the injection of additional freshwater (with roughly the same isotopic content) from Hudson Strait. The primary branch of the Labrador Current lies along the shelf break, but a significant alongshore current also follows the marginal trough (PIPER,

this issue). The complex bathymetry, with numerous channels and saddles, allows a liberal exchange to take place. Near 48°N, the inshore and offshore branches of the Labrador Current diverge with the offshore branch (90%) following the outer edge of the Grand Banks of Newfoundland while the inshore branch flows along the coast through Avalon Channel (PETRIE and ANDERSON, 1983). Some (20%) of the inshore branch then turns westward and enters the Gulf of St Lawrence while the rest flows offshore. Much of the offshore branch of the Current turns eastward at the southern tip of Grank Bank, but some continues westward as a deep "Labrador" component of the slope water off Nova Scotia (GATIEN, 1976).

Reinforced by freshwater runoff in the Gulf of St Lawrence, the coastal flow emanates from Cabot Strait into the nearshore region of the Scotian Shelf where it flows westward to the Gulf of Maine. Joining the deep slope water input through Northeast Channel, the coastal flow then exits the Gulf of Maine onto the New England Shelf. As on the Labrador Shelf, the rugged topography of the Scotian Shelf and Gulf of Maine strongly influences the path of the current and its exchange with offshore waters (SMITH *et al.*, 1978; HOUGHTON *et al.*, 1978). Some uncertainty surrounds the fate of the freshwater input to the Gulf of St Lawrence since its ^{18}O content should be quite distinct from that of the northern Labrador Sea, yet it is not detected in samples from the western Scotian Shelf or Gulf of Maine. Moreover, isotope data from the central Gulf of St Lawrence show little evidence of local runoff except in a thin surface layer (P. STRAIN, Chemical Oceanography, Bedford Institute of Oceanography, personal communication). CHAPMAN and BEARDSLEY (1989) attribute masking of the isotopic signature of the Gulf of St Lawrence runoff to thorough mixing with a much larger volume of Labrador water over the Scotian Shelf. This hypothesis requires testing.

Maximum mean surface velocities over the shelf (Fig. 1b) are generally associated with the major transports. In the West Greenland and offshore Labrador Currents speeds range from 0.4–0.6 m s^{-1}, while inshore currents in Avalon Channel and on the Scotian Shelf lie between 0.1 and 0.3 m s^{-1}.

Seasonal circulation

The hydrographic properties and longshore volume transport of coastal currents exhibit strong seasonal cycles as well as significant interannual variability which lead to inferences about freshwater sources and driving mechanisms. For instance, MYERS *et al.* (1989) have correlated seasonal salinity cycles (Fig. 3a) and residuals at Station 27 (off St Johns, Newfoundland) with similar variations in certain northern freshwater sources to demonstrate that Labrador sea ice-melt, not Hudson Bay runoff, is the primary determinant of the seasonal cycle in Newfoundland Shelf salinity, but that Hudson Bay residuals do impact its interannual variability.

Similarly SUTCLIFFE *et al.* (1976) and SMITH (1989b) have used seasonal cycles in temperature and salinity to infer that freshwater runoff into the Gulf of St Lawrence governs the seasonal but not the interannual variability on the Scotian Shelf. Moreover, DRINKWATER *et al.* (1979) and SMITH (1983b) have shown that the hydrographic cycles are associated with strong annual signals in alongshore transport. A comparison (Fig. 3b) of monthly mean transports in the Nova Scotian Current at Cabot Strait, Halifax and Cape Sable (off southwest Nova Scotia) reveals a distinct similarity when suitable lags (3 and 4 months, respectively) are applied to the Halifax and Cape Sable signals. These lags are

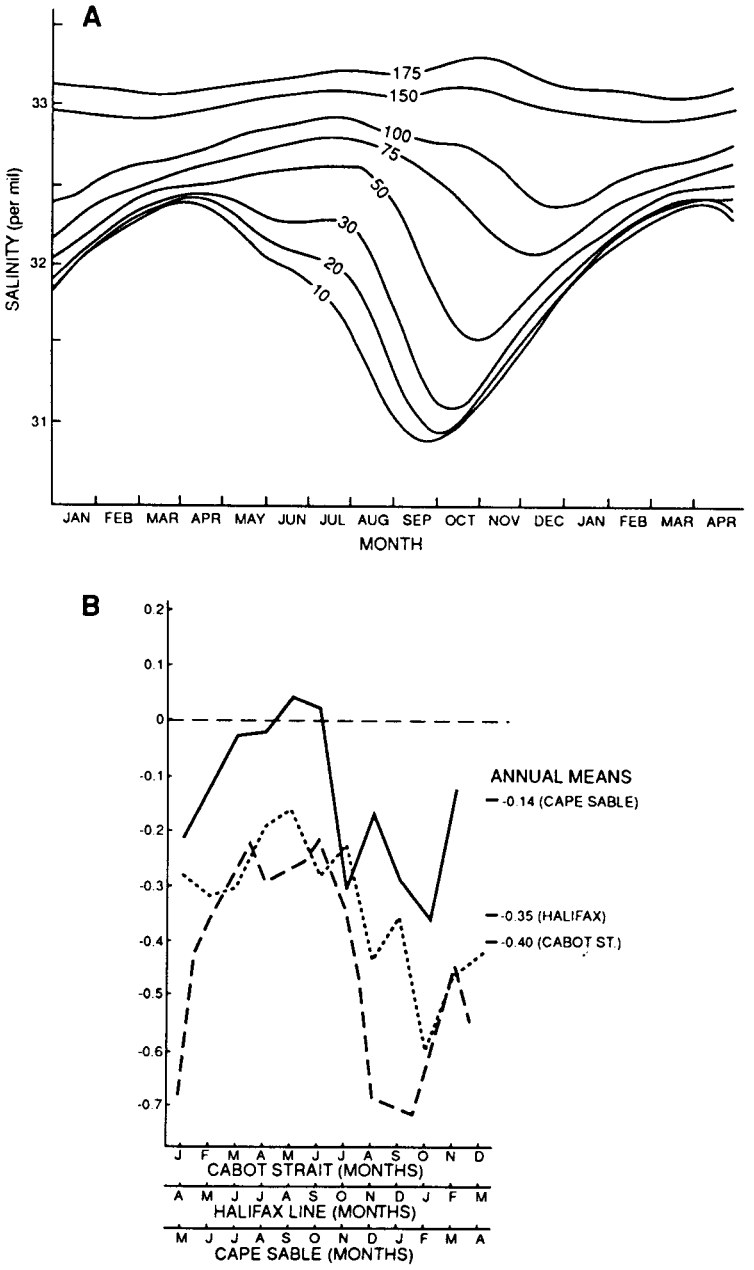

Fig. 3. (A) Seasonal salinity cycle at Station 27, off St Johns, Newfoundland, as a function of depth (from MYERS *et al.*, 1989). (B) Monthly mean alongshore transports on the Scotian Shelf including geostrophic transports from Cabot Strait (dash) and the Halifax Section (dot) (both from DRINKWATER *et al.*, 1979) and estimates from measured currents off Cape Sable (solid; SMITH, 1983b). Note that different time scales suggest 3 and 4 month lags for the Halifax and Cape Sable signals behind Cabot Strait. Annual mean transports are indicated on the right.

consistent with alongshore advection at an average rate of 6 km day^{-1}. Note that the Cabot Strait and Halifax transports are based on geostrophic estimates, whereas the Cape Sable signal is calculated from measured mean currents. This may account, in part, for the large difference in the annual mean transport through the Cape Sable section. However, another possibility is the offshore migration of the axis of the Current because of friction and/or topographic steering.

Dynamics

Using a simple diagnostic model, SMITH (1983b) concluded from observations that the primary dynamical balance for the nearshore circulation on the western end of the Scotian Shelf involves alongshore gradients in pressure (i.e. sea level) and density as well as nonlinearities associated with topographic rectification of tidal currents (LODER, 1980). By imposing a 20 mm coastal setup (with a linear cross-shelf gradient to zero at the shelf break) on the eastern (backward) boundary, he was able to obtain reasonable agreement between observed depth-averaged annual mean currents and the M_2 tidal residual circulation of a nonlinear barotropic model (Fig. 4a). Prominent features produced by tidal rectification include a clockwise gyre over Browns Bank and an inshore jet off Cape Sable. The alongshore flow off Shelburne is due primarily to the alongshore pressure gradient set by the boundary condition.

Similarly, GREENBERG and PETRIE (1988) specified boundary forcing to be one half of the observed steric height profile along a Labrador Shelf transect in order to drive a barotropic model of the mean circulation on the Newfoundland Shelf and Slope (Fig. 4b). In spite of some obvious shortcomings, such as the absence of the Gulf Stream and North Atlantic Current, comparisons with observed depth-averaged currents show some quantitative agreement. However, some features, including the position and width of the Labrador Current and the observed clockwise gyre on Flemish Cap, are not reproduced and may be attributable to baroclinic effects.

Barotropic models have also been found useful in simulating the depth-averaged mean flow driven by wind. However, care must be taken to impose an appropriate condition at the backward boundary. For example, WRIGHT *et al.* (1986) specified a coastally-trapped pressure field equivalent to that of an arrested topographic wave (equation 12a) on their eastern boundary at Halifax in order to account for wind forcing over the portion of shelf not included in their model. Because the direct effects of the forcing over the domain are small near the backward boundary, the boundary forced component of flow is dominant over the western Scotian Shelf as suggested by Fig. 2b. Hence the depth-averaged model current (Fig. 5a) compared well with the observed mid-depth current responses only when the boundary forcing was applied (Fig. 5b).

In spite of the successes of the barotropic models in simulating observed depth-averaged currents, in many instances knowledge of the baroclinic structure of the flow is essential for determining certain aspects of the flow, for example, the transport of particulate matter near the surface or near the seabed. During the CASP experiment, volume transport on the Scotian Shelf attained its seasonal maximum in December 1985, then declined slowly until the end of the experiment in early April 1986 (ANDERSON and SMITH, 1989). The four-month mean currents (Fig. 6) show that along the 100 m isobath, the flow appears to be relatively barotropic, whereas in deeper water there is significant shear over the upper 100 m of the water column.

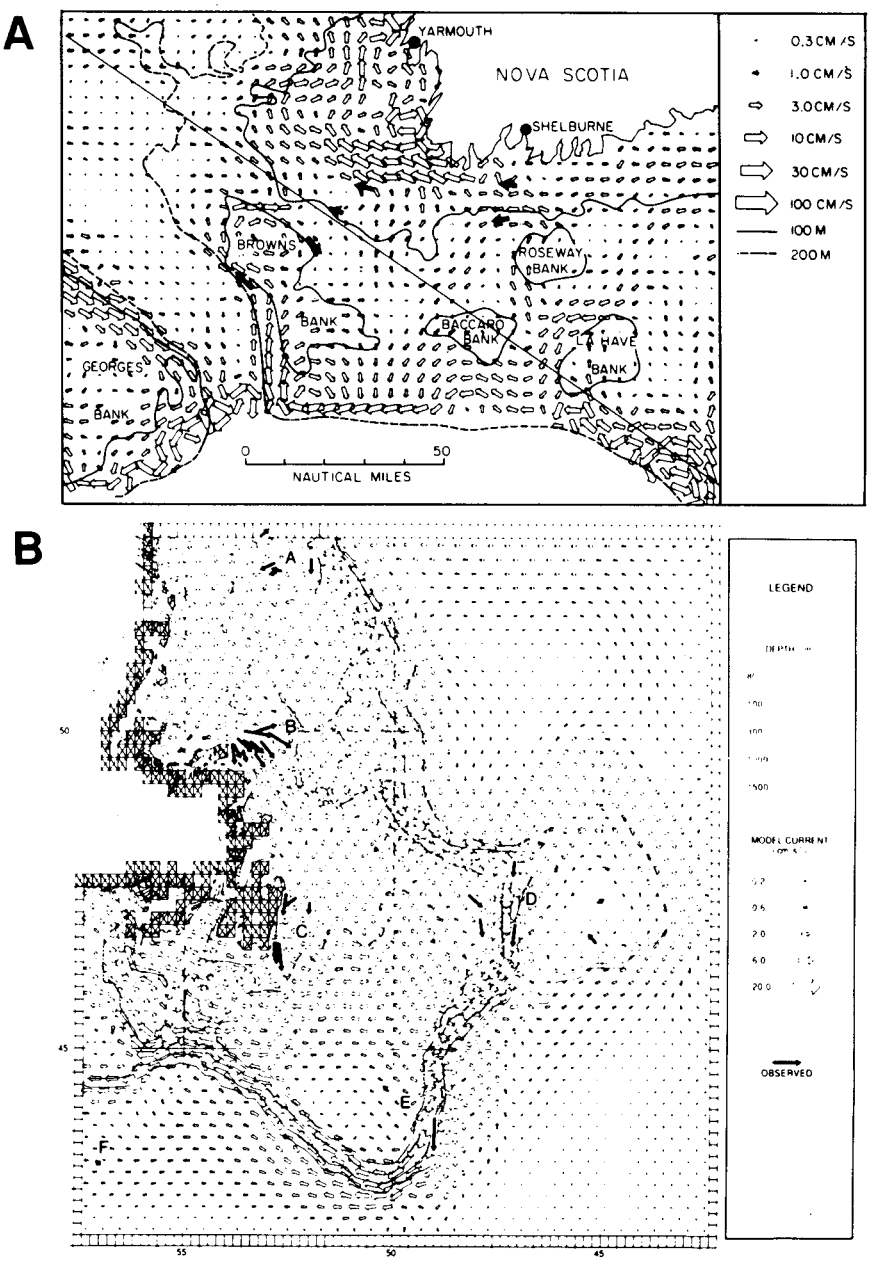

Fig. 4. Comparisons between the nonlinear, barotropic model and observations of the mean circulation. (A) Circulation in the eastern Gulf of Maine off Cape Sable, Nova Scotia. Measured currents (solid) are the depth-averaged annual means. Backward boundary of the model has been set up by 20 mm (see text; from SMITH, 1983b). (B) Circulation on the Newfoundland Shelf. Measured currents (solid) are means from longest available records from the area. Backward boundary has been raised by an amount equal to one half the dynamic height on an historical hydrographic section on the Labrador Shelf. Arrow length is proportional to the square root of the current (after GREENBERG and PETRIE, 1988).

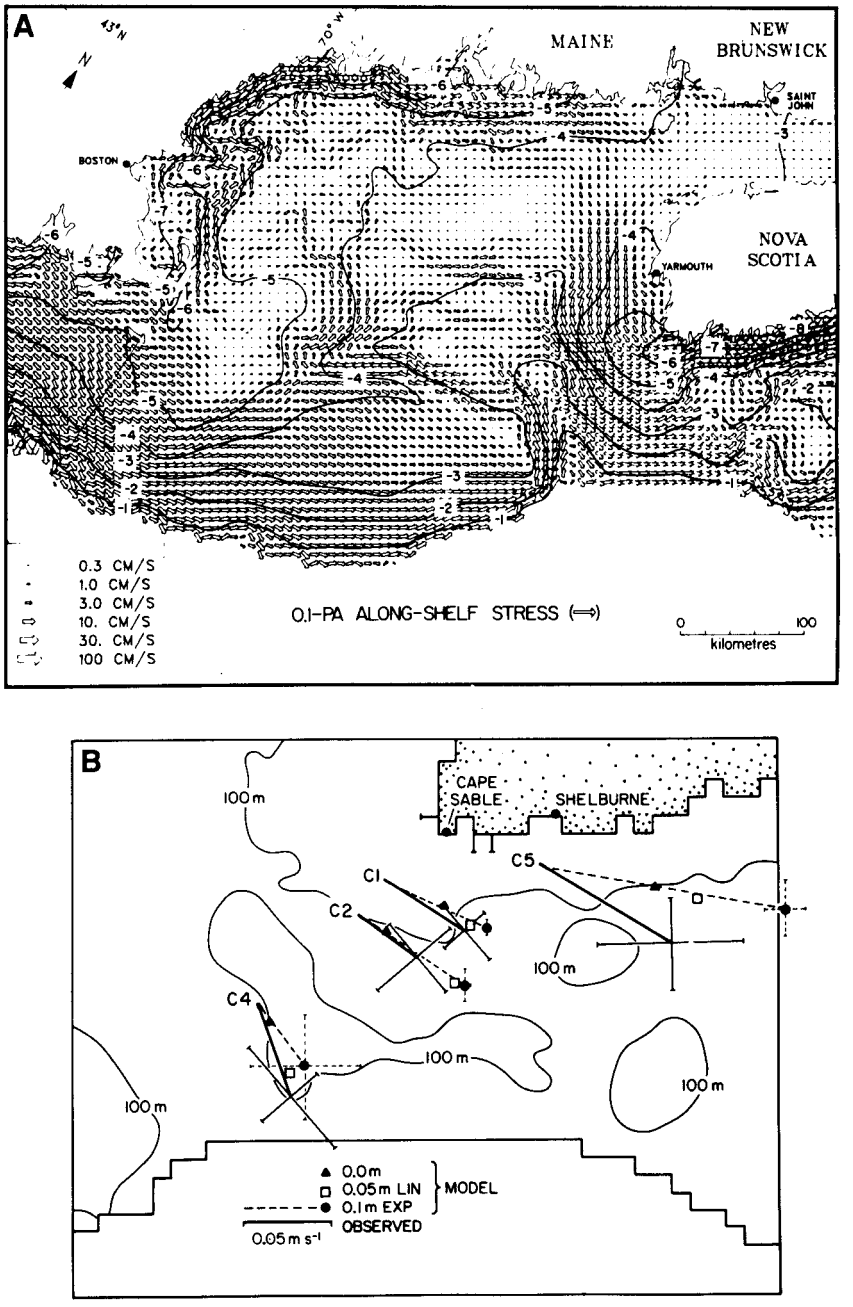

Fig. 5. (A) Predicted elevations (cm) and currents from a linear barotropic model driven by a 0.1 Pa uniform alongshelf wind stress, including a 0.1 m exponential set-down across the backward boundary. (B) Comparison of model (dash) and observed (solid) current responses off southwest Nova Scotia for a 0.1 Pa alongshelf wind stress. Predicted responses include (▲) no set-up, (●) 0.1 m exponential set-up, and (□) 0.05 m linear set-up on the backward boundary (from WRIGHT *et al.*, 1986).

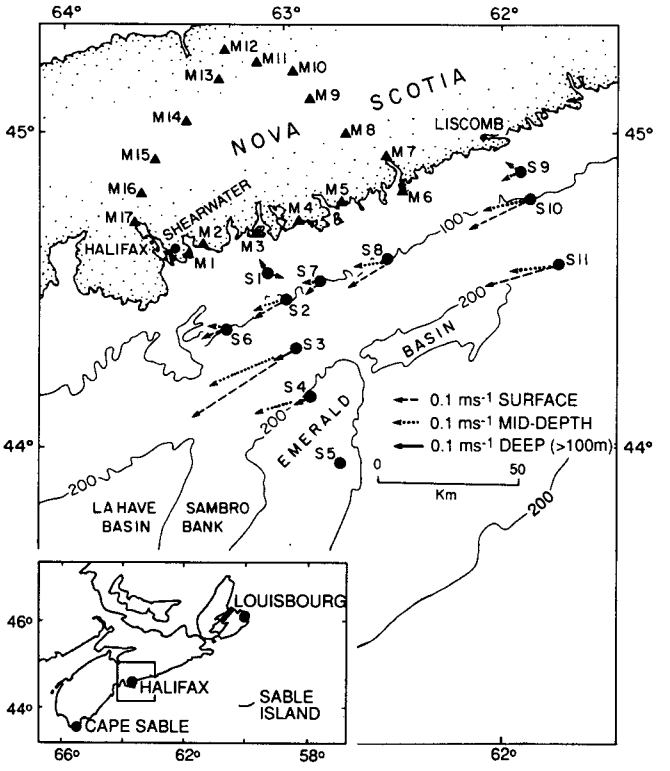

Fig. 6. Mean currents observed during the CASP field program (1 December 1985–31 March 1986) at moorings S1–S4 and S6–S11 from the surface layer (solid), mid-depth (40–100 m; dot) and deep layer (>100 m; dash). Mesoscale wind measurements were made at land-based mesonet stations (M1–M17) (from ANDERSON and SMITH, 1989). Inset shows place names for the Scotian Shelf.

In a depth-averaged sense, the maximum current lies near S3 and S11 on the 150 m isobath, roughly 45 km from the coast, whereas the flow inshore on the 60 m isobath is much weaker and shows a tendency to reverse direction at S1 on the Halifax line. Using typical average parameters for this region of the Scotian Shelf ($f = 10^{-4}\ s^{-1}$, $s = 3.5 \times 10^{-3}$, $r = 5 \times 10^{-4}\ m\ s^{-1}$, $-y = 350$ km), the cross-shore scale length (10), $L_x \cong 32$ km, estimates the offshore position of the maximum depth-averaged alongshore current for the *boundary-forced* component of the flow. However, the mean alongshore stress during CASP ($\tau^y \cong 0.04$ Pa) implies $F = \tau^y/\rho = u_*^2 \cong 4 \times 10^{-5}\ m^2\ s^{-2}$ and so $F/r \cong 0.08\ m\ s^{-1}$. With historical estimates of the alongshore transport ($Q \cong -4.0 \times 10^5\ m^3\ s^{-1}$), the ratio of boundary- to wind-forced flow at Halifax is approximately,

$$K = \frac{fQ}{2Fy} \cong 1.4.$$

According to Fig. 2b, this means that the current maximum for the combined flow lies closer to $x = 2^{1/2}L_x \cong 45$ km ($\xi = 1$), and that a current reversal is found near the S1

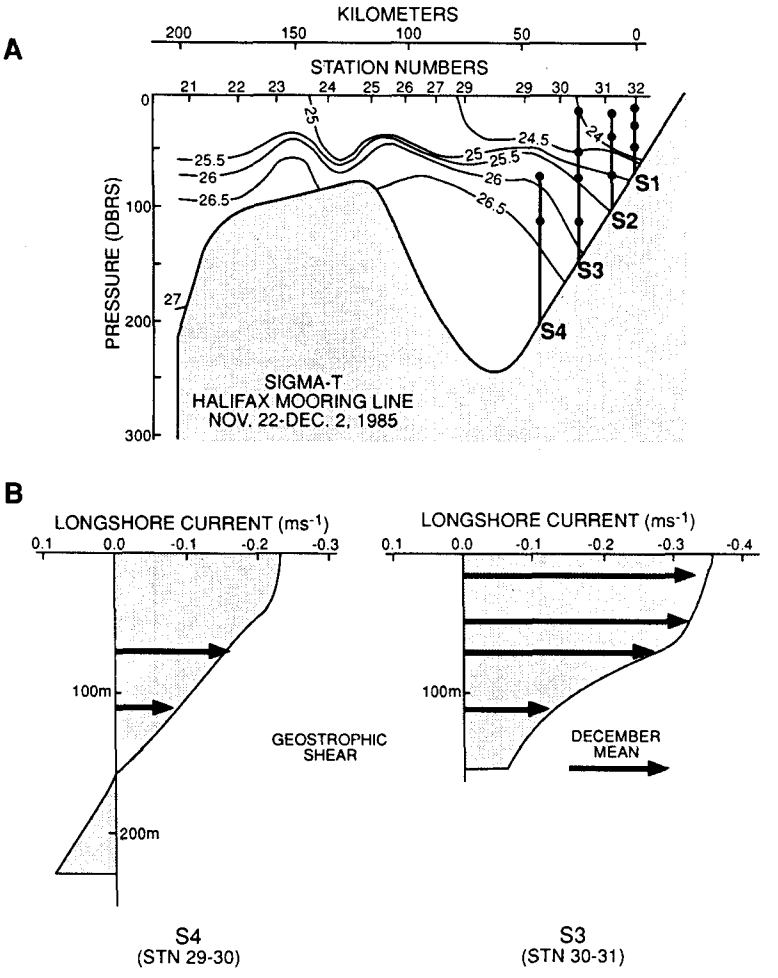

Fig. 7. (A) Cross-shelf density field on the Halifax Section in early December 1985. (B) Geostrophic velocity profiles centred on CASP moorings S4 (Stations 29–30) and S3 (Stations 30–31). Solid arrows represent December mean, measured alongshore currents.

mooring, 20 km from shore, as observed. Furthermore, on the Liscomb line, the value of K is closer to 2.0 ($-y \cong 250$ km) so that the current reversal would lie inshore from the S9 mooring on the 60 m isobath. However, though the structure of the model current field is reasonable, the peak magnitude of the longshore current ($\cong$0.04 m s^{-1}) is much smaller than observed. Reducing the bottom friction coefficient would improve that comparison, but also shift the axis of the model current further offshore. Considering the neglect of stratification and other barotropic forcing mechanisms (e.g. topographic drag asymmetries; HAIDVOGEL and BRINK, 1986), the agreement between this simple model and the CASP observations must be considered qualitative at best.

In addition, the baroclinic structure of the flow is important. The cross-shelf structure of the density field off Halifax in early December, 1985 (Fig. 7), shows a strong pycnocline at

50–100 m with steeply sloping isopycnals in the nearshore region. The geostrophic shear profiles are remarkably consistent with the measured shear determined from the December mean currents at CASP sites S3 and S4. When fit to the 70 m measured velocities, the geostrophic calculations lead to: (1) depth-averaged currents of 0.27 and 0.12 m s^{-1} at S3 and S4; and (2) significant bottom currents (order 0.10 m s^{-1}) out to the 150 m isobath which have been neglected in the historical transport estimates (DRINKWATER *et al.*, 1979). This indicates that the net volume transport at this time contains a large barotropic component, of order 1–2 times the baroclinic component. Clearly, measurements of the density field alone are inadequate for determining either the volume transport or the magnitude and direction of the near-bottom currents. On the other hand, the dynamical origin of the barotropic component of the flow is unknown. Considering the evidence for important buoyancy sources in the Labrador Sea and Gulf of St Lawrence, thermohaline mechanisms such as JEBAR are considered leading candidates for driving the mean coastal circulation.

WIND-DRIVEN VARIABILITY

The response of the Atlantic Canadian coastal ocean to transient wind forcing varies with season. The severe winter weather is due primarily to extratropical cyclones which develop along the eastern seaboard of the U.S. and propagate northeastward along the Polar Front. These storms are organized on a broad range of scales from synoptic (2000 km) to the mesoscale (20–200 km). In coastal waters, synoptic-scale atmospheric forcing is associated with subtidal variability (periods of 2–10 days) while mesoscale forcing is often linked to clockwise-rotating inertial currents (periods from 17–22 h, depending on latitude). Furthermore, surface waves generated by storm winds affect the low-frequency circulation in shallow water through their influence on bottom friction.

In summer, lighter southwesterly winds generally prevail that are punctuated by the occasional intense tropical storm (DRINKWATER, 1989). The summer water column is highly stratified and southwesterly winds favour coastal upwelling on the Scotian Shelf and shelf regions of like orientation. PETRIE *et al.* (1987b) have used satellite images to demonstrate that persistent summer winds produce a band of cold, upwelled water near the coast that subsequently forms eddies (50 km scale) through baroclinic instability of the upwelling front. PETRIE (1983) has also observed baroclinic upwelling and the Scotian Shelf break in winter.

The focus of this section is placed on the wintertime response in shallow ($\leq$100 m), well-mixed water because strong currents are developed, especially near bottom. The storm response described here is characteristic of other regions of the eastern Canadian shelf since the same storms tend to track along the coast.

Subtidal variability

As with the mean and seasonal circulations subtidal variability on the continental shelf may be driven by both local wind and boundary forcing. Energy propagates along the shelf in the "forward" direction via CTWs (GILL and SCHUMANN, 1974; CLARKE and BRINK, 1985) which are damped by friction and often scattered by topographic irregularities. On the Labrador Shelf, WEBSTER and NARAYANAN (1988) have demonstrated that CTWs generated by flow through Hudson Strait dominate the subtidal current variability in the

northern regions (e.g. Sagalek Bank), but are roughly equivalent to the local wind-forced fluctuations further south (at Nain Bank). This change in relative importance of the two forcing components with downstream distance is a consequence of the scattering and frictional decay of the CTW and the growth of the local response with downshelf distance as in the steady case (Fig. 2b). The forcing mechanism at the northern boundary is related to a Helmholtz-like resonance of the Hudson Bay/Hudson Strait system in response to differential barometric pressure fluctuations over Hudson Bay (WRIGHT *et al.*, 1987) and the flow in Hudson Strait due to along-strait wind stress (WEBSTER and NARAYANAN, 1988). Results of a linear, barotropic model similar to (1)–(6) show reasonable agreement with observed currents. Discrepancies between the model and observations are attributed to: (1) topographic irregularities; and (2) effects of stratification.

On the Scotian Shelf, SCHWING (1989a) has recently used CASP observations to demonstrate the existence of CTWs in the subsurface pressure (SSP) field. Employing multiple regression analysis in the frequency domain he was able to separate the local (L) from the nonlocal (NL) boundary forced response by using the SSP signal very near to the backward boundary (SSP^{NL} at Louisbourg, Nova Scotia; see inset, Fig. 6) as a proxy variable for the incident CTW energy. The character of the subtidal SSP response was found to be largely independent of frequency and so could be represented by the results from a single frequency band centred at 0.125 cpd (Fig. 8). The pattern of response to local alongshore wind stress (τ^y) is similar to that of the arrested topographic wave model (12a), suitably modified to include time dependence (Fig. 8, solid curve). Thus the amplitude of the SSP response at the coast increases with alongshore distance to the west (forward direction) as the response diffuses outward across the shelf. On the other hand, the amplitude of the nonlocal SSP response decreases to the west on a decay scale of order 900 km, while the phase propagates westward as expected. Estimated phase speeds at the coast are consistent with those of frictional CTW theory for idealized Scotian Shelf topography.

The regression model containing both components of local (τ^x, τ^y) and remote (SSP^{NL}) forcing accounts for over 90% of the total SSP variance in the synoptic band at Sambro (near Halifax) (Fig. 9). The relative contributions of alongshore stress and boundary forcings are roughly equal, while the effects of cross-shore stress (τ^x) are much weaker. The importance of alongshore stress relative to boundary forcing increases to the west, in accord with the steady solution (Fig. 2b).

Unlike the pressure variability, CASP current fluctuations were much less coherent with each other or with the forcing variables, particularly local wind stress (SCHWING, 1989b). In spite of some substantial contributions from remote forcing at low frequencies (periods >5 days), the amount of alongshore current variance accounted for in the multiple regression analysis ranged between 50 and 80% with the highest values found inshore. Nevertheless, the significant velocity responses at individual moorings were relatively independent of depth; the flow appears to be barotropic. Furthermore, some integral measure of consistency between SSP and alongshore current was found in the fact that the cross-shelf pressure gradients estimated from: (1) the cross-shelf difference in SSP response; and (2) the geostrophic-equivalent pressure difference derived from the cross-sectional average current response, were comparable for both the locally and remotely forced components.

The discrepancy between the spatial coherence scales of SSP and current has also been noted in the Gulf of Maine by VERMERSCH *et al.* (1979), who speculated that highly

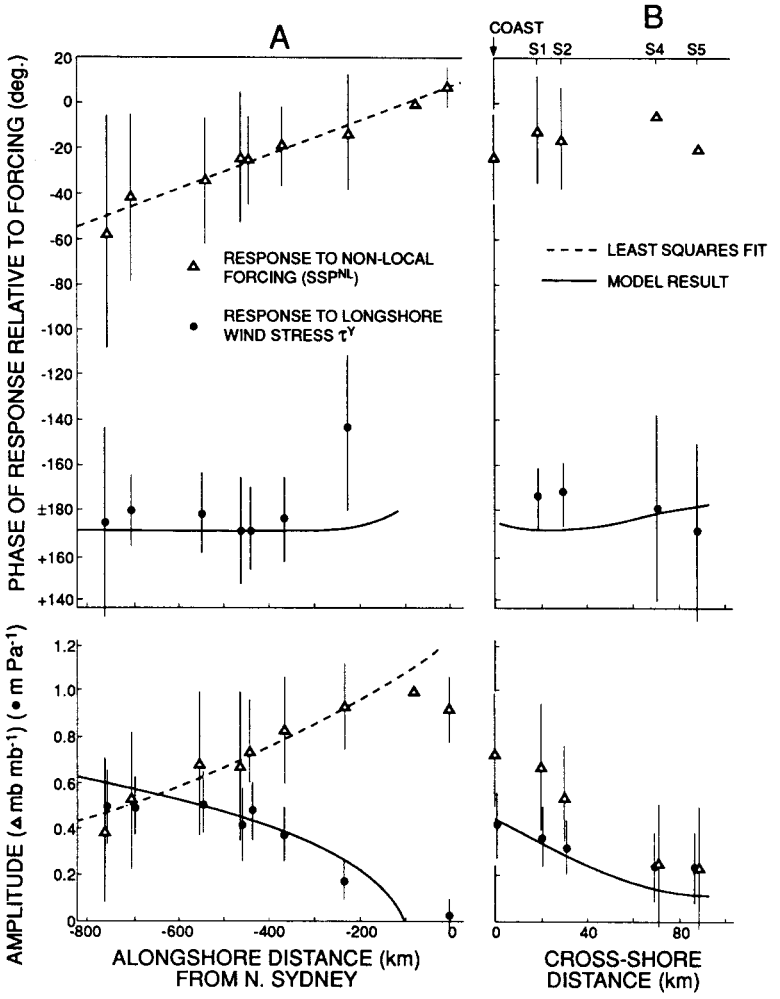

Fig. 8. Phase and amplitude of the 0.125 cpd subsurface pressure (SSP) response to Sable Island alongshelf wind stress, τ^y, and to Louisbourg SSP as a function of (A) alongshelf and (B) cross-shelf distances. Error bars are the 95% confidence limits. Solid curves represent locally forced response of a simple time-dependent model (SCHWING, 1989a) and dashed lines are fits to the nonlocal response.

irregular topography was responsible for generating mesoscale eddies in the current field. SCHWING (1989b) has used a series of simple models with idealized topographic features to demonstrate that vortex stretching, topographic steering and scattering of CTW energy, combined with strong friction, were all important mechanisms affecting the spatial variability of current more so than pressure. For quantitative comparison, he then developed a linearized barotropic model with harmonic time-dependence and realistic Scotian Shelf bathymetry (Fig. 10a). At a frequency of 0.125 cpd, the numerical results for the depth-integrated transport resulting from local (Fig. 10b) and boundary (Fig. 10c)

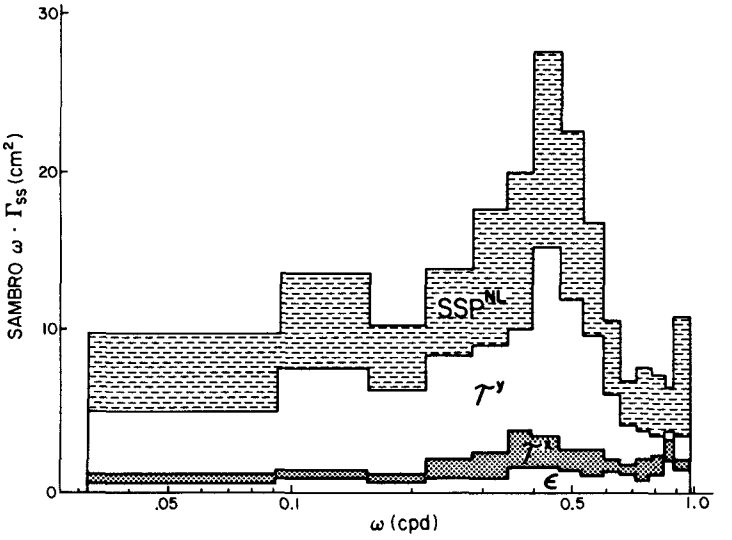

Fig. 9. Distribution of variance in Sambro SSP due to Sable Island wind stress components (τ^x, τ^y) and nonlocal forcing (SSP^{NL}). Region labelled ε represents residual error (<10%).

forcing show a rich complexity of small-scale circulations, superimposed on a background flow with many of the gross features of the idealized models (9) and (12). The alongshore stress (τ^y) applied uniformly over the domain west of Louisbourg, is maximum to the east at $\omega t = 0$ and reversing at $\omega t = \pi/2$. The response generally grows in the forward direction, with a maximum near the coast, but also shows evidence of topographic steering. As the stress reverses, closed circulation cells with scales of 50–100 km are clearly seen in association with topographic features.

The boundary forcing in Fig. 10c is in the form of a mode-1 CTW incident on the cross-shelf (backward) boundary, 140 km east of Louisbourg. The response is normalized to Louisbourg sea level, with unit (zero) amplitude at $\omega t = 0$ ($\pi/2$). For this case, the maximum transports are offshore as the flow is clearly guided away from the shallow regions. Some wave energy is deflected backward or off the shelf and the net transport decreases in the forward direction due to both scattering and frictional dissipation. Again as the flow reverses, there is evidence for small-scale residual features trapped to the topography. Another interesting aspect of the numerical model is that the solutions west of Louisbourg for higher-mode (e.g. mode-2) incident waves are very similar to that for the mode-1 incident wave, both in structure and phase speed. It appears that the higher modes are effectively scattered and dissipated by the rugged shelf bathymetry on a scale smaller than the shelf width, so that only mode-1 survives over the forward portion of the shelf. Thus the boundary-forced response is largely independent of the incident wave form.

At higher frequencies, the same qualitative picture emerges, but the flow is less influenced by topography. Detailed comparisons of model results with CASP alongshore current response (SCHWING, 1989b) show approximate agreement in amplitude and phase, especially in the nearshore region and for the remotely-forced component of flow. As

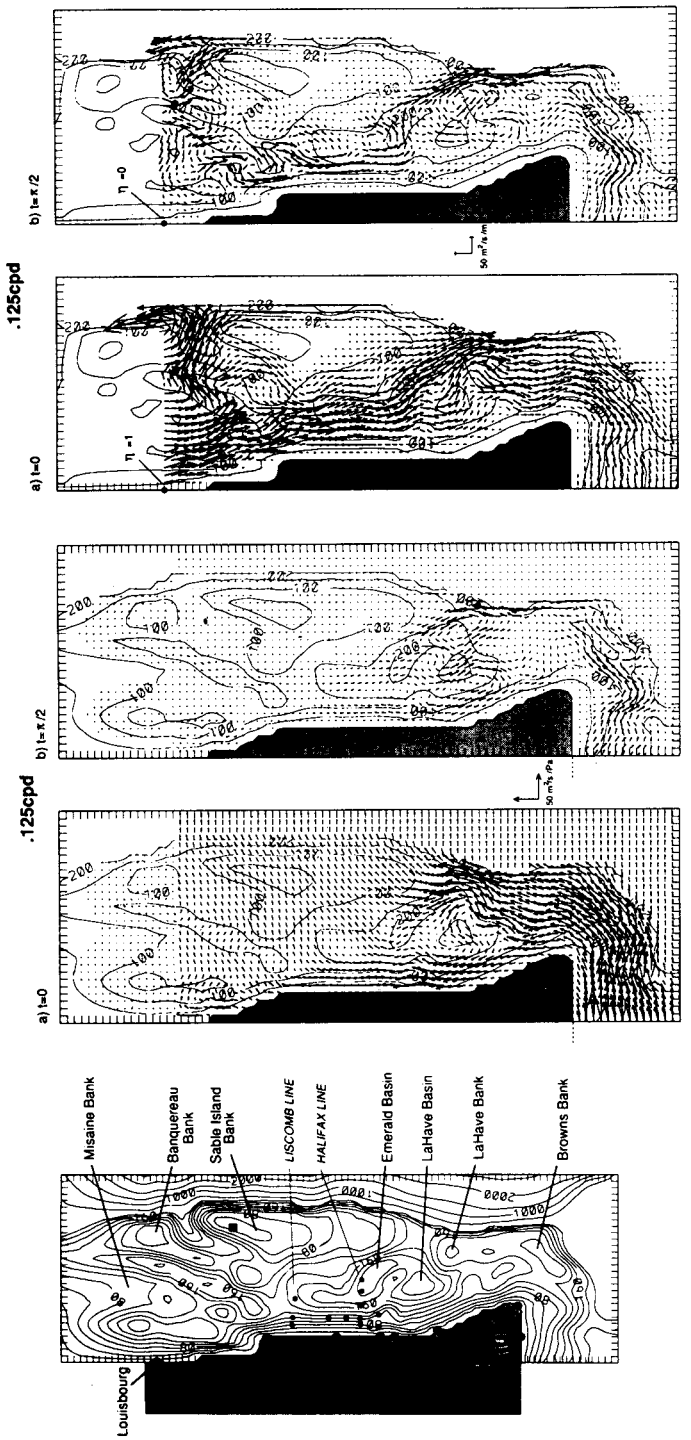

Fig. 10. Scotian Shelf model transport response to local (B) wind stress and nonlocal (C) boundary-forcings at 0.125 cpd. Wind stress is applied uniformly in the region west (forward) of Louisbourg; remote forcing is in the form of a mode-1 CTW at Louisbourg. The model domain is shown in (A) (from SCHWING, 1989b).

found for the Labrador Shelf, discrepancies in the offshore zone may be caused by baroclinic effects associated with the relatively weak wintertime stratification.

Inertial response

In the deep ocean, the large-scale response to an isolated storm consists of a forced component moving with the storm and a spreading, three-dimensional wake of inertial-gravity waves (PRICE, 1981, 1983). When the storm moves over the stratified waters of the continental shelf, however, the inertial wave field is forced to accommodate: (1) a shallow water column, where the thickness of the deep layer may be the same order as the mixed layer depth; (2) coastal boundaries, which inhibit inertial motions; and (3) frictional dissipation. The character of the inertial response on the shelf is strongly controlled by the relative magnitudes of the storm speed, U, and the characteristic speeds of the barotropic, c_0, and first baroclinic, c_1, modes of the system (KUNDU and THOMSON, 1985). DE YOUNG and TANG (1989) have demonstrated that on the outer regions of the Grand Banks of Newfoundland, isolated, intense autumn storms, for which $c_0 \gg U \gg c_1$, generate purely baroclinic inertial waves which may be simulated by an inviscid, one-dimensional, two-layer model driven by observed winds. The responses in the upper and lower layers are 180° out of phase and the inertial transport (current × thickness) is the same in both layers. However, when the scales of the forcing wind field are less well-defined, the model assumptions are violated and the comparison is degraded.

When inertial waves encounter the coast, the condition of no normal flow through the solid boundary causes scattering into other baroclinic modes such that this condition is satisfied (KUNDU, 1986). During CASP, a succession of winter storms over the Scotian Shelf drove a highly intermittent inertial current response, indicated by complex demodulation of the current velocity components at inertial frequencies (Fig. 11c,d; SMITH, 1989a). Peak amplitudes of 0.20 m s^{-1} were reached in the surface layer on the 150 m isobath [S3 (16 m), S11 (11 m); Fig. 11c] during a particularly intense storm (IOP14) on 7 March 1986. On the same isobath, deep inertial currents [S3 (110 m); Fig. 11d] were nearly as strong, but "coastal inhibition" of inertial wave energy was also evident by comparing the surface layer responses on the 60 m isobath [S1 (12 m)] with those further offshore.

To investigate the structure of the inertial response to IOP14, CASP current records were band-pass filtered at the inertial frequency and complex correlated (KUNDU, 1986) with the record from the near-surface instrument at S3 (16 m) over a 3-day period encompassing the storm event. [The magnitude of the complex correlation represents the weighted-average correlation of two vector time series, while the phase gives the average counterclockwise angle (looking downward) of the vector of interest with respect to the reference vector.] The phase on the Halifax mooring line exhibits rapid clockwise turning with depth through the pycnocline (50–70 m) indicating upward phase and downward energy propagation (Fig. 12a). Deep water currents are coherent but out of phase with the surface. However nearshore, the sharp decline of the correlation signals the inhibition of inertial wave energy.

A plan view of the surface-layer average correlation (Fig. 12b) indicates roughly onshore propagation of the rapidly decaying inertial wave. [Note however that differences in spacing of phase lines along the eastern (Liscomb) and western (Halifax) mooring lines suggest that two essentially independent estimates of phase speed exist.] An examination of the synoptic fields of the IOP14 storm (Fig. 13a) shows that peak winds over the Scotian

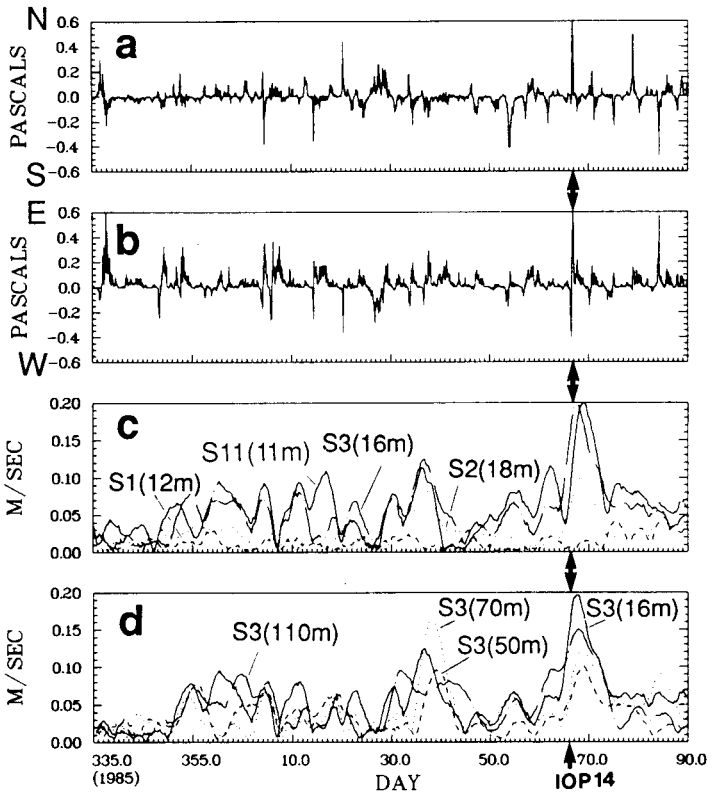

Fig. 11. Time series of Shearwater (see Fig. 6) wind stress and the amplitude of the inertial complex demodulate of the cross-shelf current component. (A) Northward wind stress; (B) eastward wind stress; (C) inertial current amplitude in the surface layer; (D) inertial current through the water column at S3. Solid arrows mark the IOP14 storm (from SMITH, 1989a).

Shelf near 1200 GMT on 7 March rotated sharply from easterly to southwesterly in association with a narrow mesoscale warm front within the storm. The mesonet estimate of the velocity of the front, $U \cong 10$ m s^{-1} to the north, is consistent with at least one estimate (8.1 ± 0.9 m s^{-1} on the Liscomb line) of the onshore propagation speed of the inertial currents (the other appears to be contaminated by proximity of the Halifax line to the storm centre; SMITH, 1989a). Furthermore, the temperature and density records reveal a baroclinic wave propagating *offshore* at $c_1 \cong 1.8$ m s^{-1} as a result of the coastal adjustment process. These features are qualitatively consistent with numerical model results of KUNDU (1986) for the response to a moving front which crosses the coast.

These analyses suggest that inertial currents near the bottom will be most important in shallow, stratified waters away from the coast (i.e. over the outer banks of the shelf). Although some details of the generating mechanism(s) remain obscure, it is clear that intense winter storms play an important role. Because of its significance to sediment transport at the seabed, it is worthwhile to examine some effects of bottom friction associated with storms.

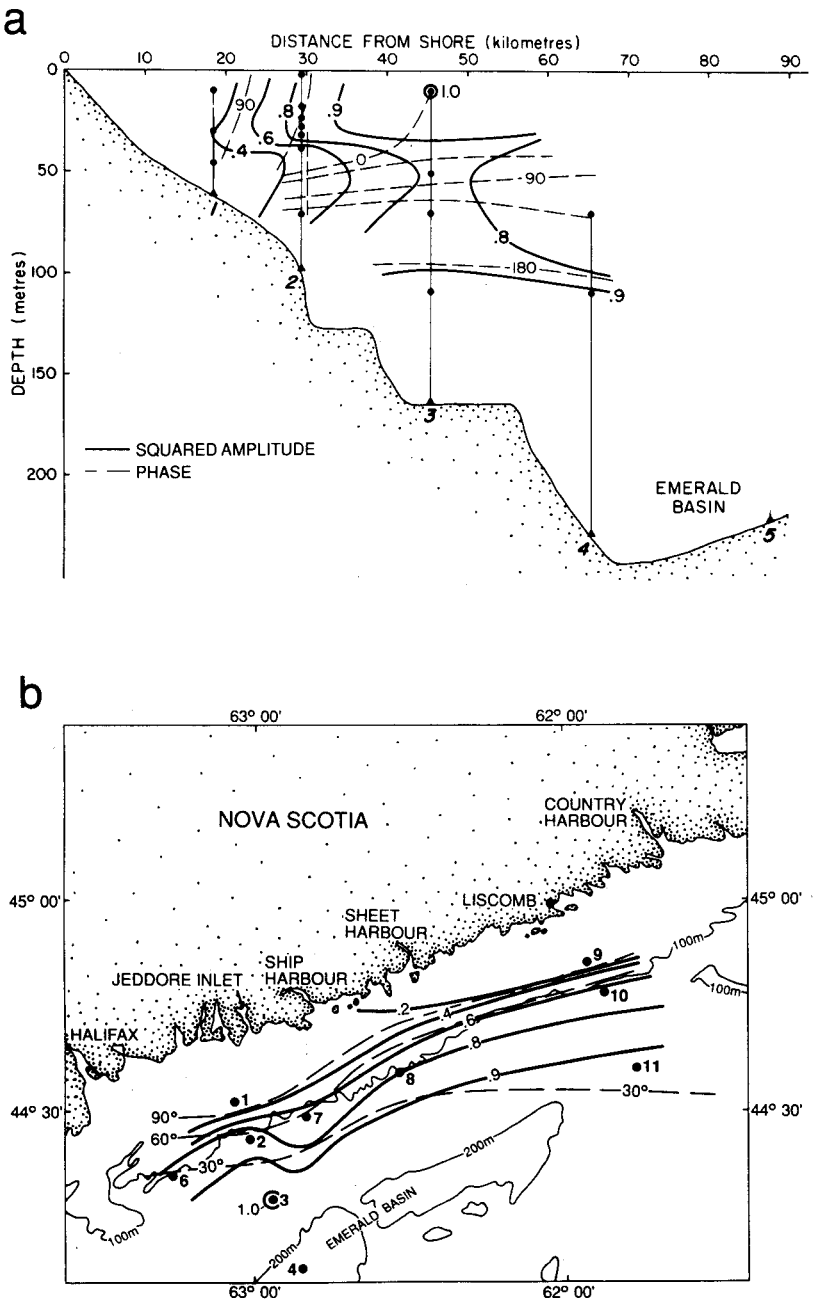

Fig. 12. Contour plot of the magnitude and phase of the squared complex correlation of currents measured during CASP IOP14. (A) Vertical section along the Halifax mooring line; and (B) plan view of the average values in the surface mixed layer (depth <40 m) (from SMITH, 1989a).

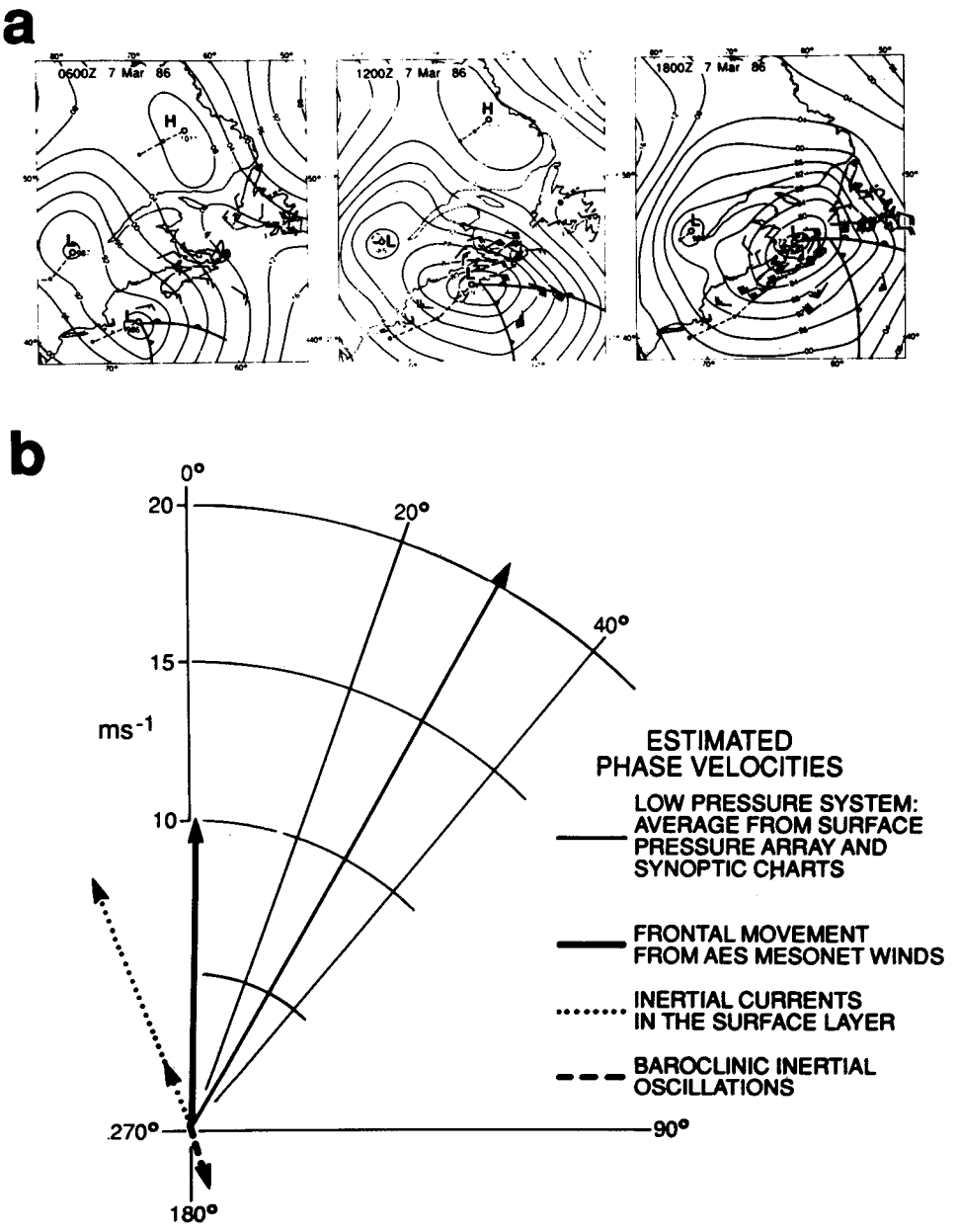

Fig. 13. (A) Synoptic weather charts showing movement of the CASP IOP14 storm across the region during 0600–1800 GMT, 7 March 1986. (B) Estimated phase velocities during CASP IOP14, including motion of the low pressure centre from surface pressure measurements, frontal velocity from mesonet winds, two estimates of onshore propagation of inertial oscillations in the surface layer, and an estimate of the baroclinic phase velocity on the Liscomb mooring line (from SMITH, 1989a).

Surface waves and bottom friction

Detailed mapping of the seabed in the nearshore region of the CASP mooring array reveals a wide variety of bottom types (sand, gravel, cobble-boulder lags, bedrock; PIPER, this issue) which lead to substantial variation in bottom roughness [10^{-4} m $< k_s <$ 1 m (grain size); $10^{-2} < k_b <$ 10 m (bedform); FORBES and DRAPEAU, 1989; FORBES *et al.*, this issue] and that creates resistance to the fluid flow above. Furthermore, during storms the bottom stresses are enhanced by the presence of surface waves which increase the apparent roughness of relatively smooth bottoms through interaction with the current within the wave boundary layer (GRANT and MADSEN, 1979). Under these conditions, it is reasonable to question the conclusion that the inhibition of inertial waves is due entirely to (inviscid) scattering of incident energy at the coastal boundary, and to consider the role of frictional dissipation in shallow water.

Surface wave measurements were made during CASP with an array of wave riders and directional wave buoys (WAVECs) in the nearshore region off Martinique Beach near Halifax (Fig. 14; DOBSON *et al.*, 1989). In the wake of the IOP14 storm, these instruments recorded significant wave heights from 1.5 to 6.0 m propagating onshore from the east and south, with characteristic periods ranging from 6 to 13 s (Fig. 15). At the same time, nearshore moorings (B1–B4) carrying Aanderaa instruments were measuring currents at 1 m above the bottom in depths ranging from 20 to 37 m as part of a sediment transport study (FORBES and DRAPEAU, 1989). Comparing these currents with those offshore in the surface layer (Fig. 16) clearly shows the shoreward decay of inertial wave energy. Inside the 60 m isobath (S1), all vestiges of the 17-h oscillation disappear and the flow mirrors the wind stress with a small but significant phase lag.

Sample calculations (following MARTEC, 1984) using the GRANT and MADSEN (1979) formulation with observed wave and current data reveal strong temporal and spatial variations of the bottom stress during IOP14, as well as extreme sensitivity to the bottom roughness scales. Near-bottom orbital wave velocities and displacement amplitudes were estimated from the directional wave spectra at the WAVEC sites and currents (u_b, 1 m above the bed) were interpolated from either the measured currents at B1–B4 or estimated deep currents at S1 and S2. The resulting time-averaged bottom shear stress, $|u_{*c}|^2$, is related to the bottom resistance coefficient, r, by

$$r(x, t) = |u_{*c}|^2/|u_b|.$$

Following FORBES and DRAPEAU (1989), the minimum stresses were obtained for a flat, immobile bed of uniform sand ($D = 0.2$ m) with nominal bed roughness of $k_b = 30\,D$. The cross-shelf profiles of $r(x, t)$ show dramatic variations (Fig. 17a). On the 100 m isobath (WC33, 30 km from shore), the resistance coefficient lies between 1 and 2×10^{-4} m s^{-1} until the 13 s waves arrive at 2400 GMT, day 66, that is, roughly 12 h after the storm centre passed over the Scotian Shelf off Halifax (Fig. 13a). At 1200 GMT, those values apply to the entire region, while at 2400 GMT, r increases shoreward by more than a factor of two. The maintenance of significant currents and large, long-period waves over the succeeding 12 h suggests that the 2400 GMT profile remains well into the following day.

When the grain (k_s) and bedform (k_b) roughness scales of the sea floor are increased over the range corresponding (approximately) to rippled sand and gravel beds (FORBES and DRAPEAU, 1989) the estimated resistance coefficients at 2400 GMT are augmented by an order of magnitude. The maximum values of k_s and k_b are attributed to large-scale,

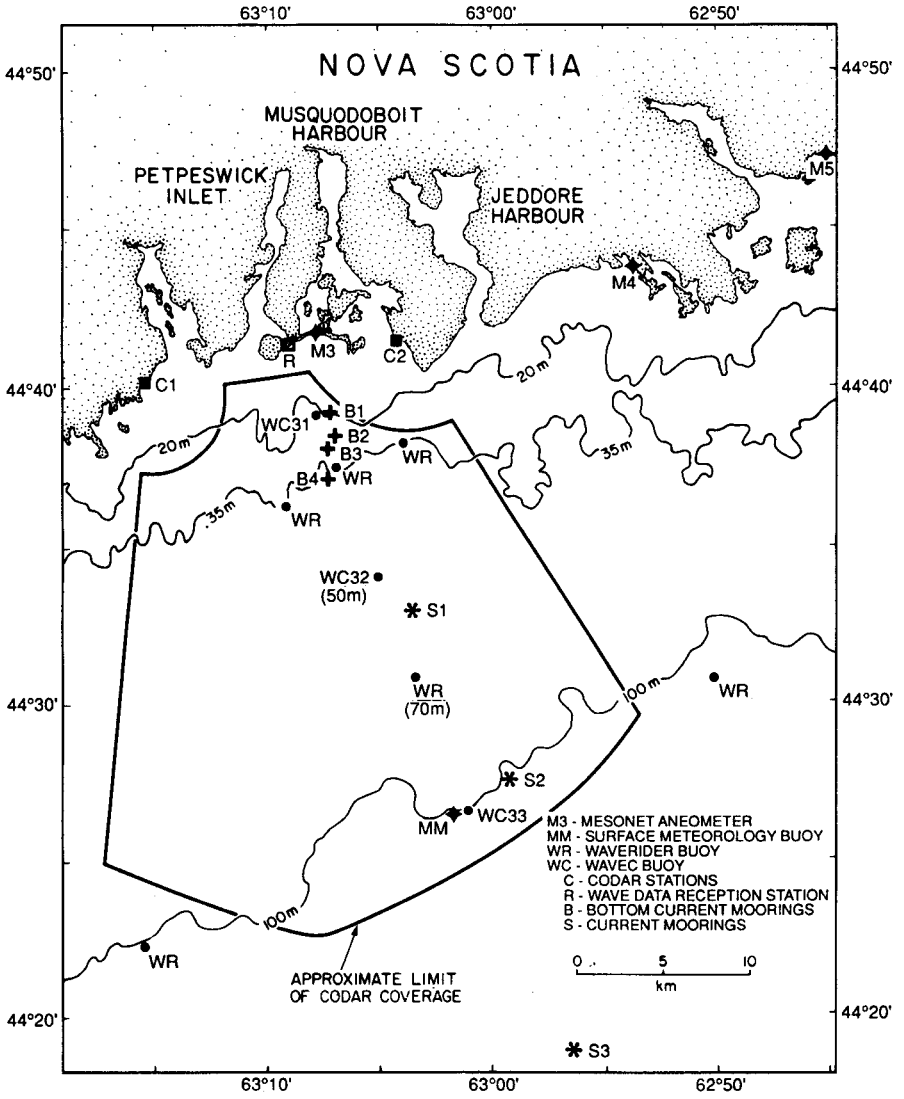

Fig. 14. Locations of CASP nearshore surface wave and current measurement arrays. Along the main line, directional wave measurements were obtained from the WAVEC buoys (WC) while currents were measured through the water column (S1–S3) and near the bottom (B1–B4). High-frequency radar (CODAR) was also used to detect surface currents and wave spectra to roughly 30 km from shore.

wave-formed ripples in gravel having wavelengths of $1 < \lambda < 3$ m and ripple heights of $0.2 < \eta < 0.4$ m. Even greater scales might be associated with observed cobble-boulder lags in the region, but their effects are not easily parameterized. For comparison with these estimates, the cross-shelf profile, $r(x)$, used by CHAPMAN (1986) and CHAPMAN *et al.* (1986) for modelling steady barotropic flow is included in Fig. 17a. This form is said to represent

a compromise between: (1) the Grant and Madsen model for 1 m, 15 s waves, and a 0.15 m s^{-1} steady current; and (2) empirical estimates of bottom friction on the shelf and slope.

The importance of friction in damping nearshore inertial energy may be estimated by comparing the inertial time scale, $T_I = f^{-1}$, to the frictional spindown time, $T_B = h/r$. For

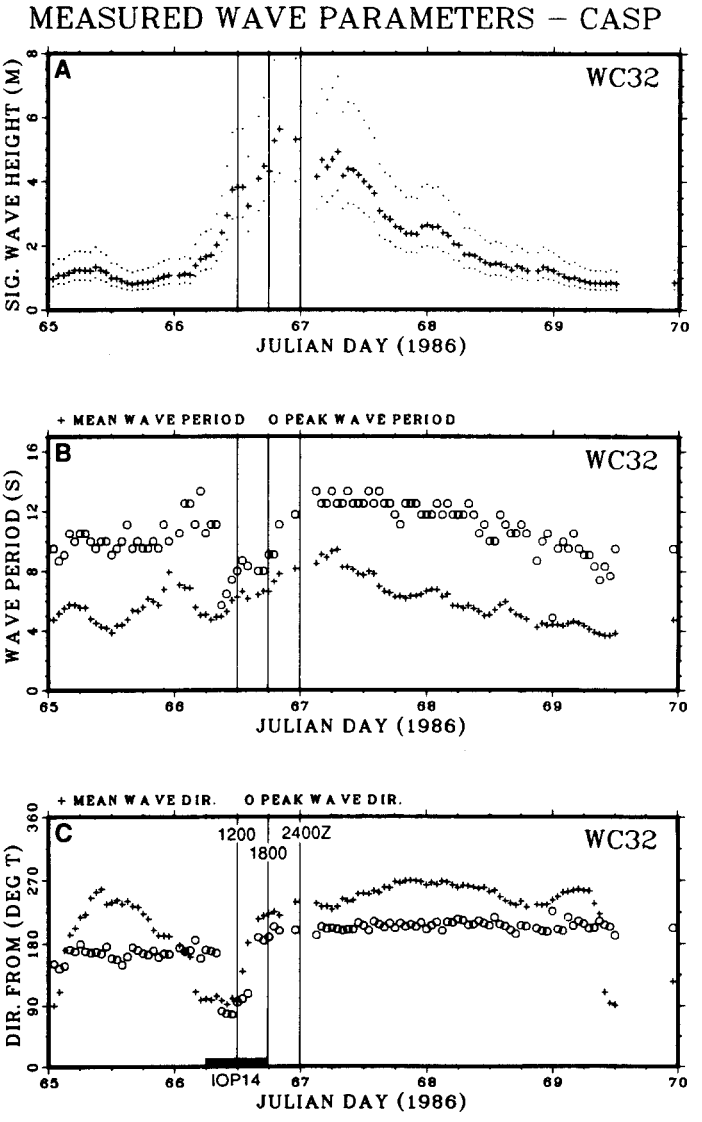

Fig. 15. Measured surface wave parameters during CASP IOP14 at the central WAVEC buoy (WC32). (A) Significant wave height; (B) mean and spectral peak wave period; and (C) mean and spectral peak wave direction. Dotted curves in (A) represent 90% confidence limits on wave height.

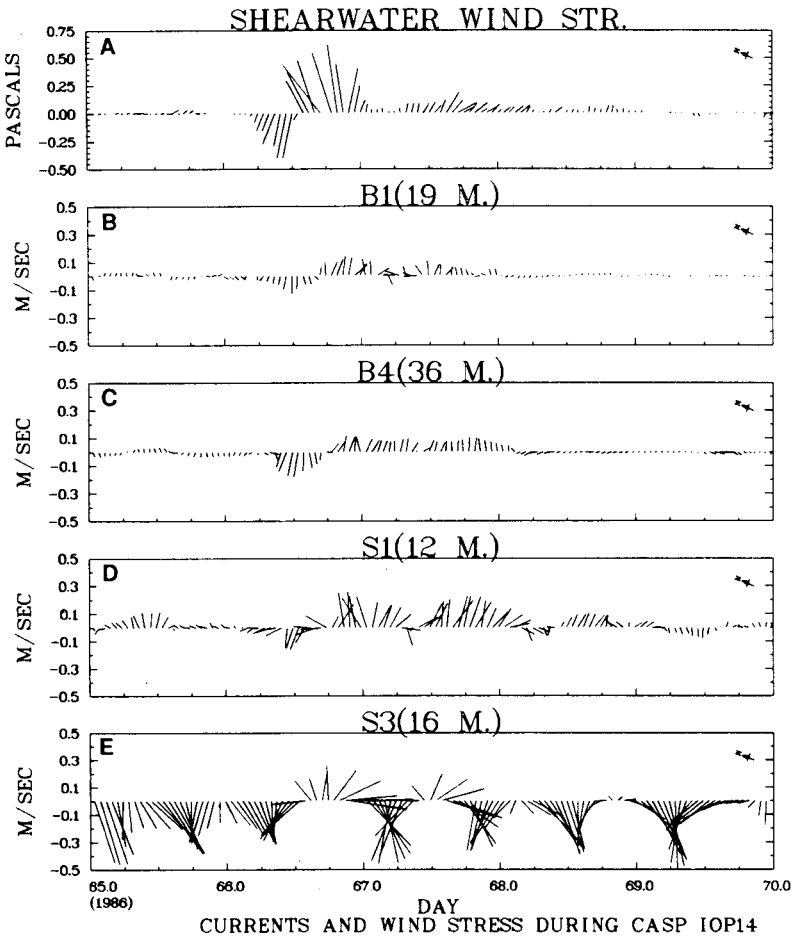

Fig. 16. Shearwater wind stress and cross-shelf distribution of currents during CASP IOP14. Currents at S1 and S3 are from the surface layer, while B4 and B1 were measured at 1 m above the bottom. Longshore direction (68°T) for current and wind is vertically upward on this page.

the flat sandy bed, the minimum value of the ratio, T_B/T_I (Fig. 17b), exceeds three for the site nearest the shore under the influence of the largest and longest-period waves. This would suggest that significant frictional damping would occur only over several inertial periods, in contrast to the observations which indicate that the inhibition process is immediate and complete. However, for a mobile bed of coarse gravel, the ratio approaches unity in shallow water, so that significant damping might occur on the inertial time scale.

Another way to gauge the importance of friction in shallow water is to consider the dynamics of the wind-driven current. If the cross-shelf current is considered small near the coast, then (2) relates the longshore current to the driving wind. Using wind data from the MINIMET buoy (similar to that in Fig. 16a) during 0600 GMT, day 66 to 0600 GMT, day 67, the longshore stress may be approximated as

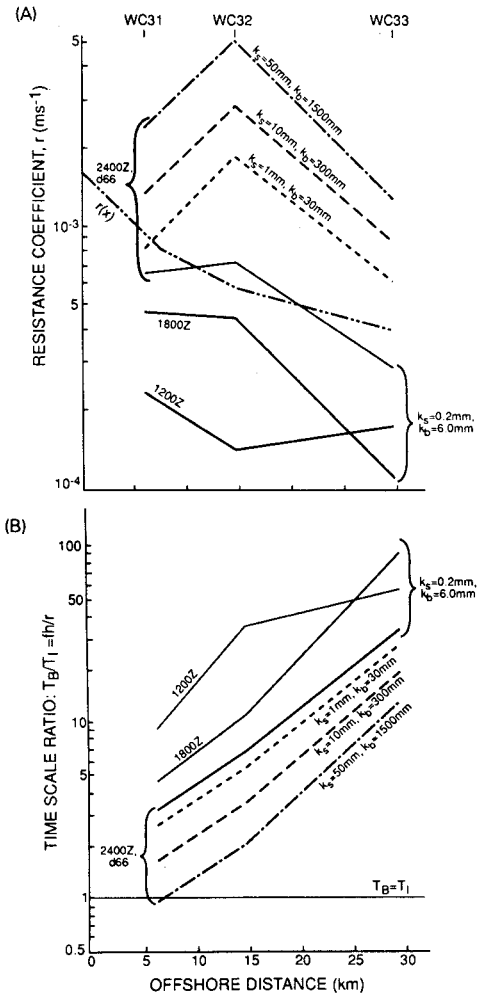

Fig. 17. (A) Cross-shelf distributions (solid curves) of the bottom resistance coefficient, r, with nominal roughness scales (k_s = 0.2 mm, k_b = 6.0 mm) as a function of time during CASP IOP14. Broken curves represent the sensitivity of the 2400 GMT cross-shelf profile to the observed range of bottom roughness scales. Also shown is the steady parameterization, $r(x)$, of CHAPMAN *et al.* (1986). (B) Cross-shelf distributions of ratio of bottom frictional spindown time, $T_B = h/r$, to inertial time scale, $T_I = f^{-1}$.

$$\tau^y = \tau_o \cos \omega t, \tag{14}$$

where $\omega \cong 2\pi$ per 24 h. With $u = 0$, (2) reduces to

$$v_t + \frac{rv}{h} = \frac{\tau^y}{\rho h} - g\zeta_y \tag{15}$$

where ζ_y is considered a constant. Neglecting transients, the solution for harmonic forcing (14) is

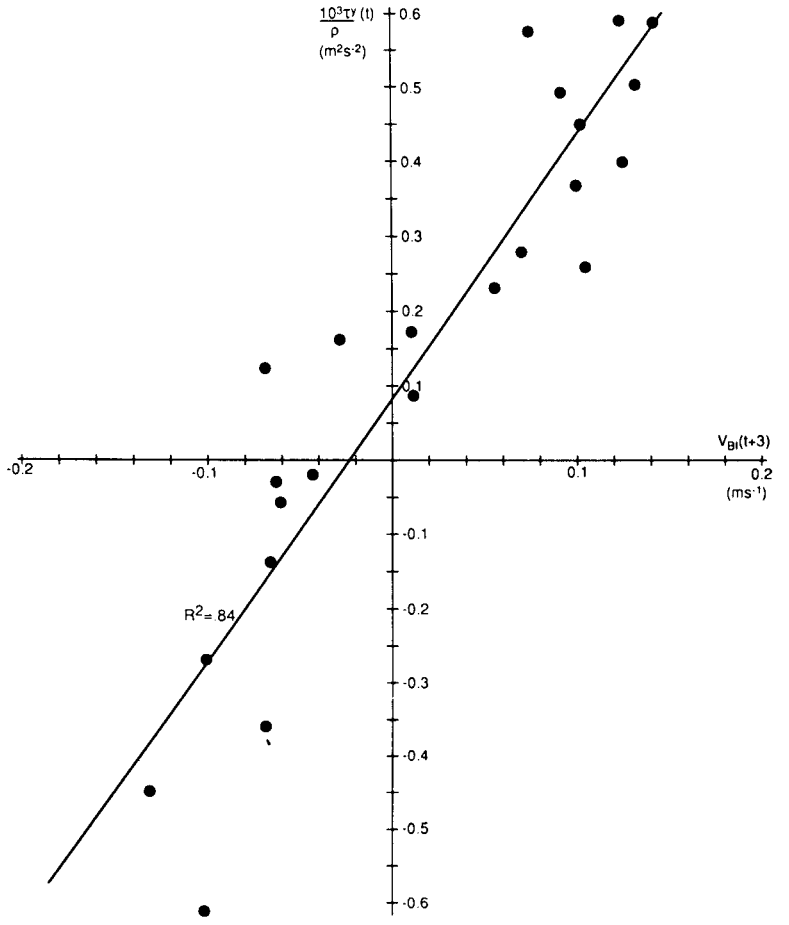

Fig. 18. Scatter plot of hourly kinematic alongshore wind stress at the MINIMET buoy (see Fig. 14) versus alongshelf bottom current at mooring B1, lagged by 3 h. Wind stress records cover the passage of the IOP14 storm (0600 GMT, day 66 to 0600 GMT, day 67). The linear regression of $10^3\tau^y(t)/\rho$ on $v_{B1}(t + 3\text{ h})$ has a regression coefficient of $R^2 = 0.839$.

$$v = \frac{\tau_o}{\rho r}\cos(\omega t - \phi) - \frac{gh}{r}\zeta_y \tag{16}$$

where $\tan\phi = \omega h/r$. Lagged correlation analysis of the MINIMET hourly alongshore stress component and near-bottom currents on mooring B1 ($h = 20$ m) indicates that the maximum correlation occurs when v_{B1} lags τ^y by 3 h. This implies that $\phi = \pi/4$, $\omega h/r = \tan\phi = 1$, so $r = 1.5 \times 10^{-3}$ m s^{-1}. Furthermore, the slope of the linear regression of $10^3\,\tau^y(t)/\rho$ against $v_{B1}(t + 3\text{ h})$ indicates that $r = 3.6 \pm 0.4 \times 10^{-3}$ m s^{-1} (Fig. 18). These two estimates are not inconsistent with those derived at 2400 GMT from the Grant and Madsen theory for waves over a rippled gravel seabed. Thus the flow along the 20 m isobath feels a resistance much greater than that associated with a sandy bottom. It is

tempting to conclude therefore that friction plays some significant role in damping inertial waves in shallow water. However, the absence of inertial oscillations at B4 on the 37 m isobath, where the friction is weaker, suggests that the rapid cancellation of the incident waves by scattering is the more likely mechanism.

Finally, according to (16), the intercept a_o, of the regression line in Fig. 18 is related to the alongshore sea level gradient by

$$\zeta_y = \frac{ra_o}{gh} \cong 6\text{–}14 \times 10^{-7}. \tag{17}$$

Estimates of this order have been obtained elsewhere on the East Coast (Scott and Csanady, 1976; Smith, 1983). In the shallow coastal zone, however, this force is dominated by those associated with surface wind and bottom stresses, as in the steady case (12).

DISCUSSION

The focus of this review has been to describe and interpret certain aspects of the structure and variability of the mean and wind-driven circulations on the continental shelves of eastern Canada. The emphasis has been on barotropic flow and the effects of topography and bottom friction on that flow. For modelling purposes, the inclusion of reasonable friction is required to reproduce the qualitative features of the circulation. Another important idea for understanding shelf circulation is the necessity to consider both the locally and remotely forced components of the circulation. In the barotropic case, these have distinctly different along- and cross-shelf structures, so that each may be dominant in a different region of the shelf. Finally, the prevalence of rugged shelf topography off eastern Canada renders the current field much less coherent than the subsurface pressure or forcing wind fields. This aspect is clearly demonstrated by the Scotian Shelf model (Fig. 10), which reveals small circulation patterns and phase variations in the time-dependent flow field (Schwing, 1989b).

Regarding the structure of coastal currents, several important physical effects have also been omitted from this discussion. Tidal friction and vertical mixing strongly influence conditions in the Gulf of Maine, for instance. Smith's (1983b) diagnostic model suggests that the bottom friction coefficient, r, associated with M_2 tidal currents on the 60 m isobath off southwest Nova Scotia may be as large as 2.4×10^{-3} m s^{-1}, consistent with the maximum values from the nearshore zone during CASP (Fig. 17a), and that horizontal density gradients maintained by gradients in tidal mixing (Loder and Greenberg, 1986) are dynamically significant. Furthermore, the three-dimensional numerical model of Tee *et al.* (1987) shows that strong tidal friction affects the vertical shear and orientation of tidal and residual currents throughout the water column in parts of the eastern Gulf of Maine. However, vertical stratification associated with seasonal buoyancy input to the region acts to reduce the vertical eddy viscosity to 20% of its value in well-mixed water.

On smaller scales, the flow of the barotropic tide generates trains of high-frequency, large-amplitude internal waves in stratified waters at sharp changes in topography, such as the shelf break or the edges of banks and ridges (Haury *et al.*, 1979; Sandstrom and Elliott, 1984). Strong bottom current pulses associated with these waves are often sufficient to resuspend sediment in the vicinity of the generation site (Butman, 1987; Boczar-Karakiewicz *et al.*, this issue).

Other aspects of stratification, such as the JEBAR mechanism (SHAW and CSANADY, 1983; HUTHNANCE, 1984) for inducing mean currents through interaction of density and topographic gradients, baroclinic modifications of CTWs, and eddy generation through baroclinic instability, have also been neglected. Unstable baroclinic eddies associated with the Labrador Current may exert a direct influence on the shelf circulation, as suggested by satellite observations (LEBLOND, 1982) and eddy statistics derived from iceberg drift (GARRETT *et al.*, 1985). In addition, the horizontal diffusion associated with an unstable eddy field may act to regulate the JEBAR forcing mechanism by smoothing the density field and reducing the baroclinic currents that drive the instability (HUTHNANCE, 1984).

With regard to CTWs, WEBSTER and NARAYANAN (1988) have attributed significant vertical phase differences in the low-frequency current response on the Labrador Shelf to the combination of local topographic and stratification effects as measured by the stratification parameter: $S = (Ns/f)^2$, where s is the local bottom slope and N is the Brunt–Vaisala frequency. SCHWING (1989b) also suggested that baroclinic effects might be responsible for discrepancies between wind-forced responses of the Scotian Shelf model and the CASP observations.

Finally, although the direct dynamical influence of the offshore, basin-scale pressure field on the barotropic shelf circulation has been largely discounted, CHAPMAN *et al.* (1986) have demonstrated that the presence of a large-scale oceanic gyre just off the shelf counteracts the offshore migration of streamlines caused by bottom friction. The result is a "dynamical barrier" which confines the coastal alongshore transport to the shelf and allows properties of the source waters to be detected far downstream. A similar process might also operate in the northern region of the Labrador Shelf where the alongshore pressure gradient associated with the circulation in the Labrador Sea would act to constrain the Labrador Current to the shelf edge as observed. Further south, where the North Atlantic Current starts to impinge on the shelf region, the alongshore pressure gradient would be weakened or reversed so that the barrier to offshore migration would be reduced. This might explain the consistent loss of surface drifters from the southern end of the Labrador Shelf (PETRIE and ANDERSON, 1983).

CONCLUSIONS

The main conclusions of this study are summarized as follows.

(a) The mean and seasonal circulations on the continental shelf of eastern Canada appear to be related to buoyancy fluxes associated with runoff and ice-melt in northern waters. The barotropic and baroclinic components of flow are of the same order on both the Labrador Shelf and the Scotian Shelf, but the dynamics of the mechanisms which give rise to them are presently unknown. Seasonal variations in the circulation and water properties (especially salinity and oxygen isotope ratio) are useful for detecting buoyancy sources. The absence of a strong ^{18}O signature of the St Lawrence freshwater runoff in the Gulf of St Lawrence and on the Scotian Shelf is puzzling and should be explored.

(b) The structure of the barotropic mean circulation and wind-driven subtidal variability are influenced by bottom friction which resists both locally and remotely forced components of the flow. These two components are distinguished by their distinctly different horizontal structures: the response to local wind is maximum near the coast and increases alongshore in the forward direction; remotely forced CTWs have maximum transports in

the deeper regions of the shelf and decay in the forward (propagation) direction. Current fields associated with both components are strongly influenced by irregular shelf topography through vortex stretching and topographic steering, while high-mode CTWs are scattered and dissipated efficiently.

(c) Inertial waves generated by intense winter storms in stratified shelf waters are strongly baroclinic over the open shelf and inhibited near the coast (within the 60 m isobath). Frictional dissipation, enhanced by surface waves and extreme bottom roughness, is capable of damping the incident energy on inertial time scales in the shallow coastal zone ($\leq$20 m), but the dominant mechanism for coastal inhibition of inertial waves appears to be scattering at the boundary. This process produces energetic inertial currents in the deep water below the winter pycnocline.

(d) The observed wind-driven response in the coastal zone during CASP lags the surface stress forcing by 3 h and is consistent with resistance coefficients, r, of order $1\text{–}4 \times 10^{-3}$ m s^{-1}. These values correspond to the large bottom roughness scales estimated for the seabed in the nearshore region of the Scotian Shelf.

Future studies of coastal circulation should be directed toward increased understanding of the baroclinic components of the mean and low-frequency circulation. The JEBAR mechanism for generating barotropic transport from the interaction of density gradients with steep topography is a prime candidate for modelling studies and comparison with existing observations. Determining the barotropic component of flow is of particular importance for sediment transport since it dictates the magnitude of the mean bottom current. Modelling the baroclinic modifications to frictional CTWs would also increase our understanding of the vertical structure subtidal variability and its implications for near bottom currents. Careful parameterization of friction in the presence of surface waves should be considered for these models.

Acknowledgements—The authors wish to acknowledge the assistance and support of members of the Coastal Oceanography Division, P.C.S., D.F.O., particularly R. R. Lively, B. Toulany and Dr C. Anderson. Dr Carl Amos kindly furnished a computer program for calculating bottom stress under waves and currents according to the Grant and Madsen formulation. Thanks also to Drs John Loder, Carl Anderson and Dan Wright for helpful comments and suggestions on the manuscript. This work was supported (in part) by the Canadian Federal Panel on Energy Research and Development (PERD).

REFERENCES

Amos C. L. and J. T. Judge (this issue) Sediment transport on the eastern Canadian continental shelf. *Continental Shelf Research*, **11**, 1037–1068.

Anderson C. and P. C. Smith (1989) Oceanographic observations on the Scotian Shelf during CASP. *Atmosphere–Ocean*, **27**, 130–156.

Beardsley R. C. and C. D. Winant (1979) On the mean circulation in the Mid-Atlantic Bight. *Journal of Physical Oceanography*, **9**, 612–619.

Boczar-Karakiewicz B., J. L. Bona and B. Pelchat (this issue) Interaction of internal waves with the seabed of the eastern Canadian continental shelf. *Continental Shelf Research*, **11**, 1181–1197.

Brink K. H. (1986) Topographic drag due to barotropic flow over the continental shelf and slope. *Journal of Physical Oceanography*, **16**, 2150–2158.

Brink K. H. and J. S. Allen (1978) On the effect of bottom friction on barotropic motion over the continental shelf. *Journal of Physical Oceanography*, **8**, 919–922.

Butman B. (1987) Physical processes causing sediment movement. In: *Georges Bank*, Ch. 13, R. Backus, editor, MIT Press, Cambridge, MA, pp. 147–162.

CHAPMAN D. C. (1986) A simple model of the formation and maintenance of the shelf/slope front in the Middle Atlantic Bight. *Journal of Physical Oceanography*, **16**, 1273–1279.

CHAPMAN D. C. and K. H. BRINK (1987) Shelf and slope circulation induced by fluctuating offshore forcing. *Journal of Geophysical Research*, **92**, 11741–11759.

CHAPMAN D. C. and R. C. BEARDSLEY (1989) On the origin of shelf water in the Middle Atlantic Bight. *Journal of Physical Oceanography*, **19**, 384–391.

CHAPMAN D. C., J. A. BARTH, R. C. BEARDSLEY and R. G. FAIRBANKS (1986) On the continuity of mean flow between the Scotian Shelf and the Middle Atlantic Bight. *Journal of Physical Oceanography*, **16**, 758–772.

CLARKE A. J. and K. H. BRINK (1985) The response of stratified, frictional flow of shelf and slope waters to fluctuating large-scale, low-frequency wind forcing. *Journal of Physical Oceanography*, **15**, 439–453.

CSANADY G. T. (1976) Mean circulation in shallow seas. *Journal of Geophysical Research*, **81**, 5389–5399.

CSANADY G. T. (1978) The arrested topographic wave. *Journal of Physical Oceanography*, **8**, 47–62.

CSANADY G. T. (1981) Shelf circulation cells. *Philosophical Transactions of the Royal Society of London*, **A302**, 511–530.

CSANADY G. T. (1982) *Circulation in the coastal ocean*, Reidel, Dordrecht, Holland, 279 pp.

CSANADY G. T. and P. T. SHAW (1983) The "insulating" effect of a steep continental slope. *Journal of Geophysical Research*, **88**, 7519–7524.

DE YOUNG, B. and C. L. TANG (1989) Storm forced baroclinic near-inertial currents on the Grand Bank. *Journal of Physical Oceanography*, **20**, 1725–1741.

DOBSON F., W. PERRIE and B. TOULANY (1989) On the deep-water fetch laws for wind-generated surface gravity waves. *Atmosphere–Ocean*, **27**, 210–236.

DRINKWATER K. F. (1989) The response of an open embayment to near-hurricane force winds. *Continental Shelf Research*, **9**, 823–839.

DRINKWATER K. F., B. PETRIE and W. H. SUTCLIFFE Jr (1979) Seasonal geostrophic volume transports along the Scotian Shelf. *Estuarine and Coastal Marine Sciences*, **2**, 17–27.

FORBES D. L. and G. DRAPEAU (1989) Near-bottom currents and sediment transport on the inner Scotian Shelf: Sea-floor response to winter storms during CASP. *Atmosphere–Ocean*, **27**, 258–278.

FORBES D. L., R. BOYD and J. SHAW (this issue) Late Quaternary sedimentation and sea level changes on the inner Scotian shelf. *Continental Shelf Research*, **11**, 1155–1179.

GATIEN M. G. (1976) A study in the slope water region south of Halifax. *Journal of the Fisheries Research Board of Canada*, **33**, 2213–2217.

GILL A. E. and E. H. SCHUMANN (1974) The generation of long shelf waves by the wind. *Journal of Physical Oceanography*, **4**, 83–90.

GRANT W. D. and O. S. MADSEN (1979) Combined wave and current interaction with a rough bottom. *Journal of Geophysical Research*, **84**, 1797–1808.

GREENBERG D. A. (1983) Modelling the barotropic circulation in the Bay of Fundy and Gulf of Maine. *Journal of Physical Oceanography*, **13**, 888–906.

GREENBERG D. A. and C. L. AMOS (1983) Suspended sediment transport and deposition modeling in the Bay of Fundy, Nova Scotia—a region of potential tidal power development. *Canadian Journal of Fisheries and Aquatic Sciences*, **40**, (Suppl. 1), 20–34.

GREENBERG D. A. and B. D. PETRIE (1988) The mean barotropic circulation on the Newfoundland Shelf and Slope. *Journal of Geophysical Research*, **93**, 15541–15550.

GARRETT C., J. F. MIDDLETON, M. HAZEN and F. MAJAESS (1985) Tidal currents and eddy statistics from iceberg trajectories off Labrador. *Science*, **227**, 1333–1335.

GRIFFITHS D. K., R. D. PINGREE and M. SINCLAIR (1981) Summer tidal fronts in the near-arctic regions of Foxe Basin and Hudson Bay. *Deep-Sea Research*, **28**, 865–873.

HAIDVOGEL D. B. and K. H. BRINK (1986) Mean currents driven by topographic drag over the continental shelf and slope. *Journal of Physical Oceanography*, **16**, 2159–2171.

HAURY L. R., M. G. BRISCOE and M. H. ORR (1979) Tidally-generated internal wave packets in Massachusetts Bay. *Nature*, **278**, 312–317.

HOUGHTON R. W., P. C. SMITH and R. O. FOURNIER (1978) A simple model for cross-shelf mixing on the Scotian Shelf. *Journal of the Fisheries Research Board of Canada*, **35**, 414–421.

HUTHNANCE J. M. (1984) Slope currents and "JEBAR". *Journal of Physical Oceanography*, **14**, 795–810.

KELLY K. A. and D. C. CHAPMAN (1988) The response of stratified shelf and slope waters to steady offshore forcing. *Journal of Physical Oceanography*, **18**, 906–925.

KUNDU P. (1986) A two-dimensional model of inertial oscillations generated by a propagating wind. *Journal of Physical Oceanography*, **16**, 1399–1411.

KUNDU P. and R. E. THOMSON (1985) Inertial oscillations due to a moving front. *Journal of Physical Oceanography*, **15**, 1076–1084.

LEBLOND P. H. (1982) Satellite observations of Labrador Current undulations. *Atmosphere–Ocean*, **20**, 129–142.

LODER J. W. (1980) Topographic rectification of tidal currents on the sides of Georges Bank. *Journal of Physical Oceanography*, **10**, 1399–1416.

LODER J. W. and D. A. GREENBERG (1986) Predicted positions of tidal fronts in the Gulf of Maine region. *Continental Shelf Research*, **6**, 397–414.

LOUIS J. P. and P. C. SMITH (1982) The development of the barotropic radiation field of an eddy over a slope. *Journal of Physical Oceanography*, **12**, 56–73.

LOUIS J. P., B. D. PETRIE and P. C. SMITH (1982) Observations of topographic Rossby waves on the continental margin off Nova Scotia. *Journal of Physical Oceanography*, **12**, 47–55.

MARTEC LIMITED (1984) SED1D: A sediment transport model for the continental shelf. Unpublished report to the Geological Survey of Canada, DSS Contract IOSC.23420-3-m753, 63 pp.

MYERS R. A., S. A. AKENHEAD and K. DRINKWATER (1989) The influence of ice-melt and Hudson Bay runoff on the salinity of the Newfoundland Shelf. *Atmosphere–Ocean*, in press.

PETRIE B. (1983) Current response at the shelf break to transient wind forcing. *Journal of Geophysical Research*, **88**, 9567–9578.

PETRIE B. and C. ANDERSON (1983) Circulation on the Newfoundland continental shelf. *Atmosphere–Ocean*, **21**, 207–226.

PETRIE, B., K. LANK and S. DE MARGARIE (1987a) Tides on the Newfoundland Grand Banks. *Atmosphere–Ocean*, **25**, 10–21.

PETRIE, B., B. J. TOPLISS and D. G. WRIGHT (1987b) Coastal upwelling and eddy development off Nova Scotia. *Journal of Geophysical Research*, **29**, 12,979–12,991.

PIPER D. J. W. (this issue) Seabed geology of the eastern Canadian continental shelf. *Continental Shelf Research*, **11**, 000–000.

PRICE J. F. (1981) The upper ocean response to a moving hurricane. *Journal of Physical Oceanography*, **11**, 153–175.

PRICE J. F. (1983) Internal wave wake of a moving storm. Part I: Scales, energy budget and observations. *Journal of Physical Oceanography*, **13**, 949–965.

SANDSTROM H. and J. A. ELLIOTT (1984) Internal tide and solitons on the Scotian Shelf: A nutrient pump at work. *Journal of Geophysical Research*, **89**, 6415–6426.

SCHWING F. B. (1989a) Subtidal response of the Scotian Shelf bottom pressure field to meteorological forcing. *Atmosphere–Ocean*, **27**, 157–180.

SCHWING F. B. (1989b) *Subinertial circulation on the Scotian Shelf: observations and models*. PhD thesis, Department of Oceanography, Dalhousie University, Halifax, Nova Scotia, Canada, 206 pp.

SCOTT J. T. and G. T. CSANADY (1976) Nearshore currents off Long Island. *Journal of Geophysical Research*, **81**, 5401–5409.

SHAW P. T. and G. T. CSANADY (1983) Self-advection of density perturbations on a sloping continental shelf. *Journal of Physical Oceanography*, **13**, 769–782.

SMITH P. C. (1978) Low-frequency fluxes of momentum, heat, salt and nutrients at the edge of the Scotian Shelf. *Journal of Geophysical Research*, **83**, 4079–4096.

SMITH P. C. (1983a) Eddies and coastal interactions. In: *Eddies in marine science*, A. R. ROBINSON, editor, Springer-Verlag, Berlin, pp. 446–480.

SMITH P. C. (1983b) The mean and seasonal circulation off southwest Nova Scotia. *Journal of Physical Oceanography*, **13**, 1034–1054.

SMITH P. C. (1989a) Inertial oscillations near the coast of Nova Scotia during CASP. *Atmosphere–Ocean*, **27**, 181–209.

SMITH P. C. (1989b) Seasonal and interannual variability of current, temperature and salinity off southwest Nova Scotia. *Canadian Journal of Fisheries and Aquatic Sciences*, **46** (Suppl. 1), 4–20.

SMITH P. C., B. PETRIE and C. R. MANN (1978) Circulation, variability and dynamics of the Scotian Shelf and Slope. *Journal of the Fisheries Research Board of Canada*, **35**, 1067–1083.

SUTCLIFFE W. H. Jr, R. H. LOUCKS and K. F. DRINKWATER (1976) Coastal circulation and physical oceanography of the Scotian Shelf and Gulf of Maine. *Journal of the Fisheries Research Board of Canada*, **33**, 98–115.

TEE K. T., P. C. SMITH and D. LEFAIVRE (1987) Modelling and observations of the residual current off southwest Nova Scotia. In: *Three-dimensional models of marine and estuarine dynamics*, J. C. J. NIHOUL and B. M. JAMART, editors, Elsevier, Amsterdam, pp. 455–470.

TEE K. T., P. C. SMITH and D. LEFAIVRE (1988) Estimation and verification of tidally-induced residual currents. *Journal of Physical Oceanography*, **18**, 1415–1434.

VERMERSCH J. A., R. C. BEARDSLEY and W. S. BROWN (1979) Winter circulation in the western Gulf of Maine: Part 2. Current and pressure observations. *Journal of Physical Oceanography*, **9**, 768–784.

WANG D. P. (1982) Effects of continental slope on the mean shelf circulation. *Journal of Physical Oceanography*, **12**, 1524–1526.

WEAVER A. J. and W. W. HSIEH (1987) The influence of buoyancy flux from estuaries on the continental shelf circulation. *Journal of Physical Oceanography*, **17**, 2127–2140.

WEBSTER I. and S. NARAYANAN (1988) Low-frequency current variability on the Labrador Shelf. *Journal of Geophysical Research*, **93**, 8163–8173.

WRIGHT D. G. (1986) On quasi-steady shelf circulation driven by along-shelf wind stress and open-ocean pressure gradients. *Journal of Physical Oceanography*, **16**, 1712–1714.

WRIGHT D. G. (1989) On the along-shelf evolution of an idealized density front. *Journal of Physical Oceanography*, **19**, 532–541.

WRIGHT D. G. and J. W. LODER (1988) On the influences of nonlinear bottom friction on the topographic rectification of tidal currents. *Geophysical and Astrophysical Fluid Dynamics*, **42**, 227–245.

WRIGHT D. G., D. A. GREENBERG, J. W. LODER and P. C. SMITH (1986) The steady-state barotropic response of the Gulf of Maine and adjacent regions to surface wind stress. *Journal of Physical Oceanography*, **16**, 947–966.

WRIGHT D. G., D. A. GREENBERG and F. G. MAJAESS (1987) The influence of bays on adjusted sea level over adjacent shelves with application to the Labrador Shelf. *Journal of Geophysical Research*, **92**, 14610–14620.